NTNU – Trondheim
Norwegian University of
Science and Technology

Dynamic Response of Flexible Pipes Considering Different Damping Models

Xueying Liu

Marine Technology
Submission date: June 2014
Supervisor: Svein Sævik, IMT

Norwegian University of Science and Technology
Department of Marine Technology

MASTER THESIS SPRING 2014

for

Stud. tech. Xueying Liu

Dynamic Response of Flexible Pipes considering different damping models

Dynamisk respons av fleksible rør med alternative dempningsmodeller

Flexible pipe response is governed by significant hysteresis in the bending mode related to friction between layers. To perform global dynamic analysis this can be handled in two ways:
1. Using the physically correct non-linear moment curvature representation of the pipe in the global model leading to long simulation times
2. Establish an equivalent viscous damping coefficient and use a linear global model

The project work focus on models for investigation the above and is to be carried out as proposed below:

1. Literature study, including flexible pipe technology focusing on the mechanical response and associated design criteria. This is also to include the techniques used to perform global and local response analysis (ensuring that the relevant design criteria are met) including non-linear finite element methods and non-linear time-domain analysis techniques with focus on the methods applied in computer programs such as ORCAFLEX, RIFLEX, SIMLA and BFLEX.
2. Define a riser scenario in terms of water depth, vessel geometry, vessel RAO, pipe cross-section properties, hydrodynamic coefficients and environmental conditions.
3. Define a cross-section model in Bflex to calculate the cross-section characteristics in terms of axial-force versus strain, torque version torsion and moment versus curvature as a function of water depth.
4. Establish alternative models in SIMLA assuming different moment-curvature relations and perform non-linear, regular wave dynamic analysis to investigate the dynamic response.
5. Perform irregular/regular wave analysis for the same cases to investigate the differences in response between the two models
6. Conclusions and recommendations for further work

The work scope may prove to be larger than initially anticipated. Subject to approval from the supervisors, topics may be deleted from the list above or reduced in extent.

In the thesis the candidate shall present his personal contribution to the resolution of problems within the scope of the thesis work

Theories and conclusions should be based on mathematical derivations and/or logic reasoning identifying the various steps in the deduction.

The candidate should utilise the existing possibilities for obtaining relevant literature.

Thesis format
The thesis should be organised in a rational manner to give a clear exposition of results, assessments, and conclusions. The text should be brief and to the point, with a clear language. Telegraphic language should be avoided.

The thesis shall contain the following elements: A text defining the scope, preface, list of contents, summary, main body of thesis, conclusions with recommendations for further work, list of symbols and acronyms, references and (optional) appendices. All figures, tables and equations shall be numerated.

The supervisors may require that the candidate, in an early stage of the work, presents a written plan for the completion of the work.

The original contribution of the candidate and material taken from other sources shall be clearly defined. Work from other sources shall be properly referenced using an acknowledged referencing system.

The report shall be submitted in two copies:
- Signed by the candidate
- The text defining the scope included
- In bound volume(s)
- Drawings and/or computer prints which cannot be bound should be organised in a separate folder.

Ownership
NTNU has according to the present rules the ownership of the thesis. Any use of the thesis has to be approved by NTNU (or external partner when this applies). The department has the right to use the thesis as if the work was carried out by a NTNU employee, if nothing else has been agreed in advance.

Thesis supervisors:

Prof. Svein Sævik, NTNU
Dr. Naiquan Ye, Marintek

Deadline: June 10th , 2014

Trondheim, January, 2014

Svein Sævik

Abstract

Flexible pipe is a layered structure composed of plastic and steel materials. Under a large bending moment, the pipe layers may slide relative to each other due to internal friction. The moment curvature relationship for the flexible pipe is a tri-linear curve. Under cyclic bending moment, a hysteresis loop will be formed in the moment curvature curve. The area of the loop is the energy loss due to the internal friction. This thesis is aimed to study the effects of hysteresis damping on the global analysis of the flexible riser.

To begin with, a review on the flexible pipe technology and nonlinear finite element method is performed. Then a local analysis is carried out in BFLEX to obtain the cross sectional characteristics. Then the global analysis is conducted to study the responses of the flexible riser in terms of the curvature, moment and axial force. From the study, slip behavior only occurs at the hang off part of the riser. For the rest part, pipe layers stay in the stick regime, meaning there is no energy loss due to the internal friction. Therefore for the global analysis of the flexible riser, there is no need to further study the equivalent linear damping models.

In addition, the influence of linear and nonlinear bending models on the global response of the riser is investigated. It is found that the current standard industrial practice, namely applying the linear bending model with the full slip bending stiffness, gives an over conservative response prediction. It is therefore recommended to use the physically correct nonlinear moment curvature relationship for the global analysis of flexible riser.

Preface

This master thesis is carried out in the department of Marine Technology in Norwegian University of Science and Technology (NTNU) for obtaining the degree of Master of Science in Marine Technology.

I would like to give my deepest appreciation to Prof. Svein Sævik at NTNU. He gave the lectures on Marine Operation during my first semester and raised my interest in flexible pipes technology. During this thesis, Prof. Svein Sævik explained the related theories and methods to me with great intelligence and enthusiasm. In addition, he continuously provided me guidance on the application of finite element codes BFLEX and SIMLA. He also encourages me warmly when I have achievements and difficulties.

Besides, I own great thanks to my co-supervisor Dr. Naiquan Ye at MARINTEK. He plays an important role in helping me plan and organize the work. On the weekly meetings, we have both educating and inspiring discussion on my topic.

Finally, I would like to thank all my friends in NTNU for the joyful days we had together.

Xueying Liu

Trondheim, June 2014

Content

List of figure

List of Table

Nomenclature

Latin letters

a	Parameter in S-N curve
A_j	Cross section area of layer j
A_t	Cross section area of the wire
c	Damping coefficient
C	Tangential material stiffness
c_{eq}	Equivalent damping coefficient
D	Fatigue damage
dof	Degree of freedom
E	Elastic modulus
E	Green strain tensor
EA	Axial stiffness
EI_s	Bending stiffness in stick regime
EI_{e1}	Bending stiffness in stick-slip regime
EI_{e2}	Bending stiffness in full slip regime
f	Volume force vector
F_f	Filled factor
F_d	Linear viscous damping force
G_i	Unit vector
GI	Torsional stiffness
K	Stiffness matrix

L	Length of the pipe
m	Parameter in S-N curve
M_1	Torsional moment in x direction
M_2	Bending moment in y direction
M_3	Bending moment in z direction
M_c	Start slip bending moment
M_d	Linear damping moment
M_f	Full slip bending moment
n	Total number of wires
n_i	Number of stress cycles under sea state i
n_j	Number of wires in layer j
N	Weighted function of displacement interpolation
Na	Number of tensile layers
Ni	Number of stress cycles to failure
Nr	Number of pressure resisting layer in pipes
P_{int}	Internal pressure
P_{ext}	External pressure
P_i	Probability of one sea state
q_1	Shear force per unit length
q_{1c}	Shear capacity
q_3	Pressure line load
Q_1	Axial force in x direction

Q_2	Axial force in y direction
Q_3	Axial force in z direction
R	Radius of the pipe
R_{int}	Internal radius of the pipe
R_{ext}	External radius of the pipe
r	Position vector after deformation
R	Position vector before deformation
S	Stress range
t	Surface traction
T_e	Effective tension
T_w	Wall tension
u	Displacement vector
u_i^0	Displacement along the centerline X^i
$\mathbf{u_\theta}$	Torsional displacement
$\mathbf{u_x}$	Axial displacement
$\mathbf{u_y}$	Transverse displacement in y direction
$\mathbf{u_z}$	Transverse displacement in z direction
W_0	Energy loss due to hysteresis damping
W_d	Work done by linear damping moment
X_1	Shear force

Greek Letters

α	Lay angle
μ	Friction coefficient
κ	Curvature of wires
ρ	Material density
ψ	Angular coordinate in the pipe cross section
σ	Stress tensor of Cauchy stress
θ	Prescribed rotation
β_2	Global curvature at the cross-section center
β_c	Slip curvature
$\rho_{\min}$	Minimum bending radius
ε_{ij}	Strain on surface which is normal to i and pointing to the j direction
ε_d	Tolerance criteria
ν_a	Passion ratio
σ_0	Stress tensor of initial stress
σ_{ij}	Stress acting on surface which is normal to i and pointing to the j direction
$\rho_{\min}$	Minimum bending radius
$\delta_{\lim}$	Permissible elongation of the outer sheath
θ_i	Rotation with respect to axes i
$\mathbf{v_s}$	Local longitudinal dofs

1 Introduction

Flexible pipe technology has experienced a fast development during the past 20 years with the increased exploitation of offshore oil and gas reservoirs. As the development of oil field enters deeper water, riser technology faces new challenges such as large vertical displacement and complicated sea environment. Because of the advantages of flexibility, easy installation, good dynamic performance, corrosion and high pressure resistance, flexible risers are widely utilized in the current oil and gas exploitation projects. To accommodate for the large motion of the topsider floater, various flexible riser configurations are developed[1].

1.1 Motivation

The characteristic of an unbonded flexible pipe is that the pipe layers are able to slide relative to each other. Therefore under a large bending moment, the pipe layers will experience the status from stick to slip due to the internal frictions between layers. The moment curvature relationship of the flexible pipe is nonlinear and the curve will form into a hysteresis loop. The area of the loop corresponds to the energy loss caused by hysteresis damping[2].

To perform global dynamic analysis, the damping in bending modes can be handled in two ways:

1. Using the physically correct nonlinear moment curvature relationship of the pipe in the global model which leads to long simulation time.
2. Establish an equivalent viscous damping coefficient and use a linear global model.

This thesis is aimed to study the influence of using different damping model on the global response of the riser.

In addition, the influence of linear and nonlinear bending models on global analysis of the riser is also to be studied in this thesis.

1.2 Scope of work

The thesis is carried out as the following:

- **Chapter 2**: introduces the flexible pipe technology include the flexible pipe characteristics, mechanical properties and design criteria.
- **Chapter 3**: reviews the theories on nonlinear finite element analysis with focus on the methods applied in computer programs SIMLA and BFLEX.
- **Chapter 4**: discusses the influence of hysteresis effects in bending mode on the dynamic response of the riser. Firstly, a local analysis is conducted to obtain the cross sectional characteristics of pipes. Next the global analysis is carried out to study the bending response of the riser.
- **Chapter 5**: investigates the global responses of riser under different bending models. Three linear bending models are compared with the physically correct nonlinear bending model. The accumulated fatigue damage is used as the criterion.
- **Chapter 6**: summarizes the conclusions reached in this thesis and proposes recommendations for future work.

2 Flexible Pipe Technology

Flexible pipes have been successfully utilized in the offshore oil industry. Compared to the rigid steel riser, flexible riser allows large deformation to accommodate the motion of topside floater as well as the unevenness of seabed. Therefore flexible pipes are extensively applied as flowlines and flexible risers. In addition, flexible pipes are easier to be transferred and installed compared to rigid pipes.

In this chapter, the characteristics of pipelines, their mechanical properties, failure modes and design criteria will be introduced.

2.1 Introduction to flexible pipes

2.1.1 Flexible pipe definition

A flexible pipe is made of a composite of metallic and polymer layered materials and allows large deflections. The characteristics of flexible pipes include[3]:

- Low bending stiffness and high axial stiffness
- Multiple helical armouring layers
- polymer outer sheath-sealing
- Allow low bending radius

There are two types of flexible pipes: bonded pipes and unbonded pipes. The bonded pipes are only used in short sections such as jumpers. In bonded pipe, the steel reinforcement is

integrated and bonded to a vulcanized elastomeric material so the layers cannot slide relative to each other. The unbonded pipes can be applied into pipelines with length of several hundred meters. The unbonded pipe consists of separate unbonded polymeric and helical reinforcement layers, which allow the relative movement between layers. This thesis is aimed to study the hysteresis damping effects which is related to the slip behavior in the pipe. Therefore unbonded pipes will be used in the future analysis.

2.1.2 Flexible pipe cross section components

The cross section of flexible pipe contains several layers. Each layer has its specific function. For a typical flexible pipe configuration as Figure 1, the following main layers are included[3, 4]:

- **Carcass** is a flat steel plate in the corrugated profile. Since during the installation and operation, the pressure barrier or other layers may be broken and the annulus is water filled, therefore the carcass must have the ability to resist the full water external pressure. However, the carcass does not need to resist the internal pressure.
- **Internal pressure sheath** is pressure tight sheath to isolate internal and external fluid.
- **Pressure armour wire** partially supports the internal sheath to resist the internal pressure loads and also resists the radical compression. The lay angle of the wire is close to 90.
- **Tensile armour** resists axial force, torque and pressure end-cap force. It is manufactured in rectangular high strength metallic wires with the lay angle within 20-60 degrees.
- **External sheath** avoids sea water and other objects to enter the internal layers. It prevents the inner layers from corrosion, abrasion and other mechanical damage.

Figure 1 Flexible pipe components[5]

2.1.3 Flexible riser system

Flexible riser is composed by flexible pipes that connect the topside structure and the subsea equipment. The flexible riser is exposed to the dynamic loads from the vessel motions as well as the environmental loads.

The main function of the flexible riser is to transfer fluids and gas from seabed to the surface platforms. It can be utilized for production, exportation and injection. The design of riser system depends on the environmental conditions, water depth and the surface platforms.

Flexible riser configuration

Flexible riser is designed to absorb the large motion of floater by changing the riser's geometry. Due to its low elastic modulus, flexible riser exhibits good performance in withstanding large dynamic displacements. Depending on the properties of riser, water depth, and motion of the topside floater as well as the environment conditions, flexible riser is designed into many configurations[6]. The most common riser configurations are shown as Figure 2.

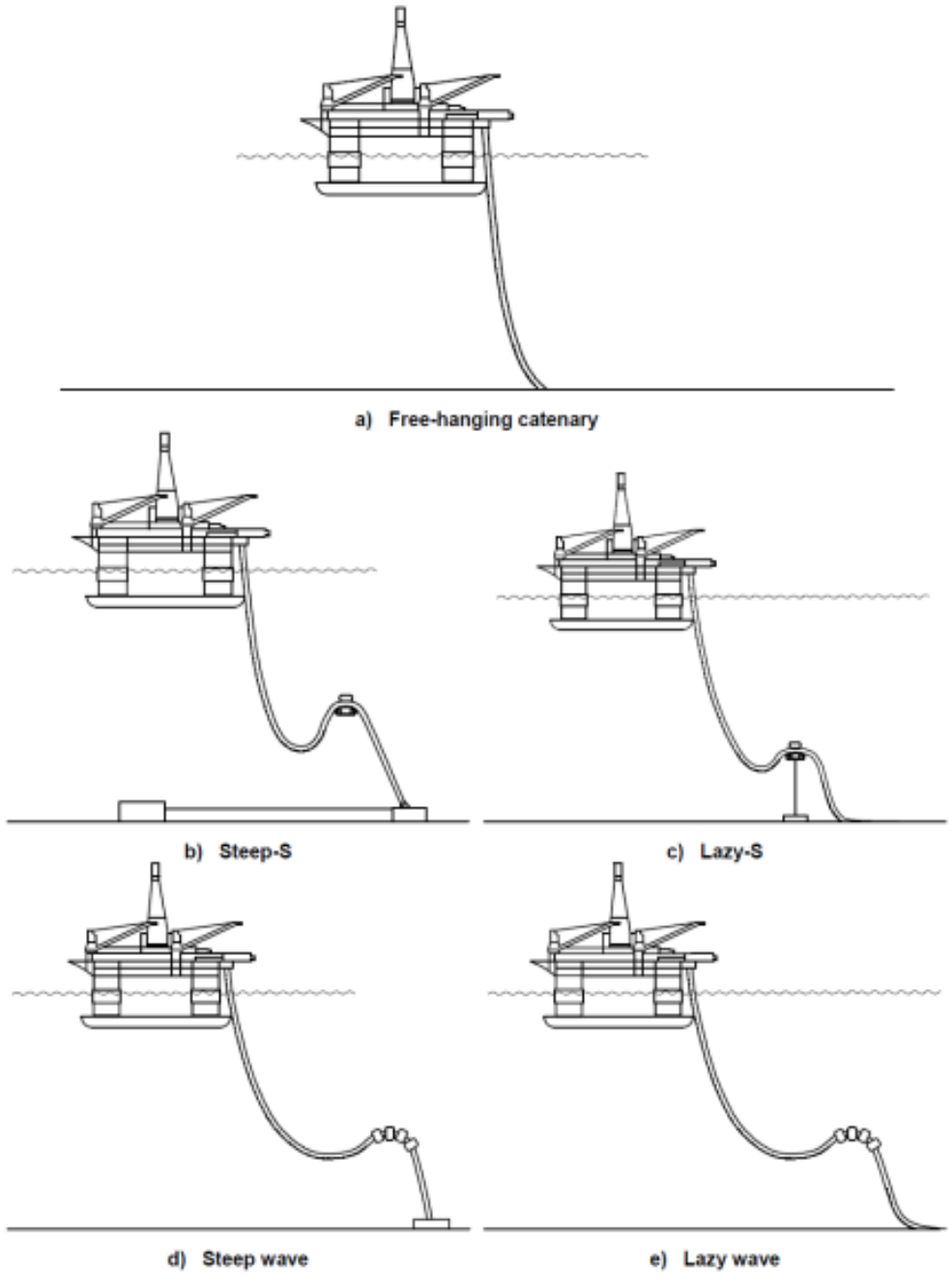

Figure 2 Flexible riser configurations[3]

The free hanging catenary configuration is the simplest configuration with the advantage of easy and cheap installation. It is widely applied on the topside floaters with low to moderate movement. The riser may face the danger of local buckling or 'bird caging' if the downward movement is large.

The lazy wave configuration is achieved by equipping buoyancy elements at the lower part of the riser. Therefore the large motions of the floater will be effectively absorbed by the hog

part of the riser. The touch down point will then be protected and the top tension will be reduced. The challenge for lazy wave configuration is the overbending at the hang-off part and near touch down point.

Steep wave configuration is similar to the lazy wave configuration except that it is vertically connected to a riser base at the seabed. Since there are fewer interfaces with the seabed, a larger motion of the riser is allowed. However, its installation is more complex and the large tension force between the riser and the riser base may lead to failure.

The lazy S and steep S configurations are to lift the riser by a subsea buoy instead of a series of buoyancy elements. It could make the layout more compact and a larger top motion is allowed. Meanwhile, the buoy stability may be a potential danger if the riser is heavy or the buoy is flooded.

Flexible riser component

Flexible riser should be strong enough to withstand the high tension force as well as flexible enough to resist the bending moment. The following key components of flexible riser are discussed to ensure the structural safety and functionality of the riser[7].

- Riser joints: mechanical connectors installed on the ends of the pipes so that pipes are connected to compose a riser.
- Buoyancy modulus: buoyancy elements attached to the flexible riser to lift up the riser. The material for construction needs to ensure a low buoyancy loss during a long term.
- Bending stiffener: component installed on the top of riser considering the hang-off part will experience high bending radius. It is utilized to increase the stiffness of riser and prevent the riser from over-bending failure.
- Bending restrictor: component also to prevent over-bending of riser at top and end connections. It is made of a hard plastic material.

2.2 Mechanical responses of flexible pipes

The wires in the pipe section are manufactured into a helical configuration which introduces initial torsion and curvature, as shown in Figure 3. The loading components in the flexible pipe could be sorted into axisymmetric loads and bending according to their effects on pipe deformation. In addition, damping and fatigue behaviors of flexible pipe will also be discussed.

The analytical solutions for axisymmetric and bending loads are based on the work of Prof. Svein Sævik's[8, 9] and will be introduced below.

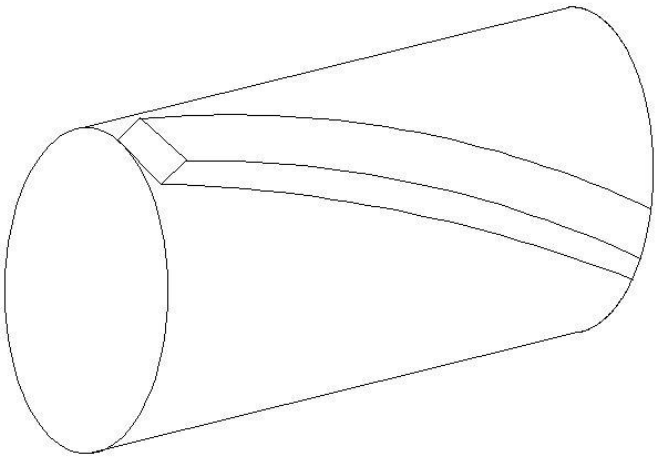

Figure 3 Initial torsion and curvature[4]

2.2.1 Axisymmetric load

Axisymmetric load does not change the cylindrical shape of the pipe. It includes tension, torsion, internal and external pressure (assuming no buckling or collapse occur). For axisymmetric loading, the axial stress along the wires will be the dominate stress since the wires lie in a helix way. The stress component from local bending and torsion will be insignificant and can be neglected.

Axial force

The analysis of long and thin wires is based on the curved beam theory. For axisymmetric loading, the shear force and bending moment in wire could be neglected. Assuming that the cylindrical shape is kept during deformation and no buckling or collapse occurs, the wire model is simplified as Figure 4. The contact pressure line load q_3 is thereby calculated as

$$q_3 = \kappa_2 Q_1 = \frac{\sin^2 \alpha}{R} Q_1 \tag{2. 1}$$

where κ_2 is the curvature in y direction, Q_1 is the axial force in the wire and α is the lay angle.

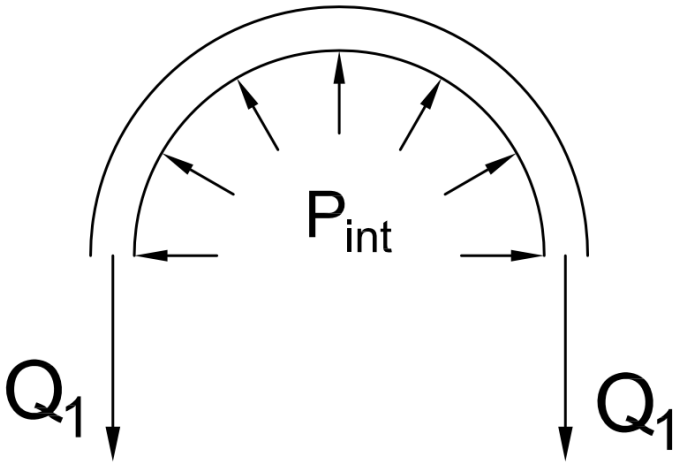

Figure 4 Illustration of pressure line load

The axial loads are assumed to be carried by the steel layers. Since the lay angle for the pressure spiral is close to 90 °, the axial loads are primarily taken by the tensile armour layer. To achieve the equilibrium, the internal tension force should balance the true wall tension as

$$\sum_{j=1}^{N_a} n_j \sigma_{11j} A_j \cos \alpha_j = T_w = T_e + \pi p_{\text{int}} R_{\text{int}}^2 - \pi p_{ext} R_{ext}^2 \tag{2. 2}$$

where N_a is the number of tensile layers, n_j is the number of wires in layer j, A_j is the cross section area, T_e is the effective tension force, T_w is the true wall tension and σ_{11j} is the axial stress in layer j. The stress in the tensile armour is estimated by the tension force divided by the effective area, as

$$\sigma_t = \frac{T_\omega}{nA_t \cos\alpha} \tag{2. 3}$$

where A_t is the cross-section area of the wire, n is the total number of wires.

The axial strain should account for the overall strain of pipe, the radical strain and the torsional displacement. The axial stiffness of two layered pipe can be obtained assuming no torsion coupling

$$EA = nEA_t \cos\alpha(\cos^2\alpha - \nu_a \sin^2\alpha) \tag{2. 4}$$

where ν_a is the passion ratio and defined as $\nu_a = -\frac{u_3}{R\varepsilon_p}$. In most cases, ν_a equals to 0.2 for the standard non-bonded pipes.

Axial stiffness is dominated by the tensile armour layers. It should be noted that radical contraction of the helix structure softens the stiffness. Based on tests, relationship between axial force and axial strain can be assumed to be linear and the equivalent damping ratio is less than 3%. The equation (2.4) is reliable for predicting axial tension but not reliable for axial compression.[10]

Torsion

Excessive torsion during pipe installation will cause 'birdcaging' failure. The torsional moment M_t will be balanced by the internal moment which is caused by the axial force in the tensile armour.

$$\sum_{j=1}^{N_a} n_j \sigma_{11j} A_j R_j \sin\alpha_j = M_t \tag{2. 5}$$

Thus σ_{11} and ε_{11} could be obtained given the torsional moment. By neglecting the overall strain and radical motion effects in the axial strain and consider only the overall torsion ε_{11}, the torsional stiffness can be evaluated as

$$GI_t = nA_t ER^2 \sin^2 \alpha \cos \alpha \quad (2.6)$$

Internal and external pressure

Excessive internal pressure will lead to bursting of the pipe. It is usually assumed that plastic layers and carcass only transmit pressure. Internal pressure is carried primarily by the tensile armour and the pressure armour layers. The pressure difference is balanced by the axial force as

$$\sum_{j=1}^{N_r} \frac{n_j \sigma_{11j} A_j \sin^2 \alpha_j}{R_j \cos \alpha_j} = 2\pi (p_{\text{int}} R_{\text{int}} - p_{ext} R_{ext}) \quad (2.7)$$

where Nr is the number of pressure resisting layers, R_{int} is the internal radius and R_{ext} is the external radius. For pipes, the bursting pressure is determined by the hoop pressure and the endcap pressure. Hoop pressure is the radical pressure contributions from tensile armour and pressure armour. The endcap pressure only comes from the tensile armour. The design bursting pressure should be smaller than both hoop and endcap pressure. Otherwise bursting may occur anyway. As long as the internal pressure and pipe is well designed, bursting is not a big problem for flexible pipe.

2.2.2 Bending

For fatigue analysis due to bending moment, the stress variation magnitude, ΔS is significant and the crack can occur everywhere. Then all the forces and moments that could contribute to the stress variation magnitude should be taken into account.

The most important feature of a flexible pipe is that the layers are able to slide against each other. Under a large bending moment, the pipe layers will experience the status from stick to slip due to the internal friction. Therefore the moment of the pipe does not vary linearly with the curvature. Under the cyclic bending moment, a hysteresis loop will form in the moment curvature relationship. The area of the loop corresponds to the energy that is consumed by internal friction during this process. This way of energy loss is called hysteresis damping.

Moment curvature relationship of pipe

The moment curvature relationship is a tri-linear curve, as shown in Figure 5. Different regimes of the curve are discussed in the following.

1) Regime I-stick regime

When the pipe is bent into a small curvature, no slip occurs between layers because the shear force is smaller than the internal friction force. Moment increases linearly with the curvature and the bending stiffness, EI_s is quite high in this stick regime.

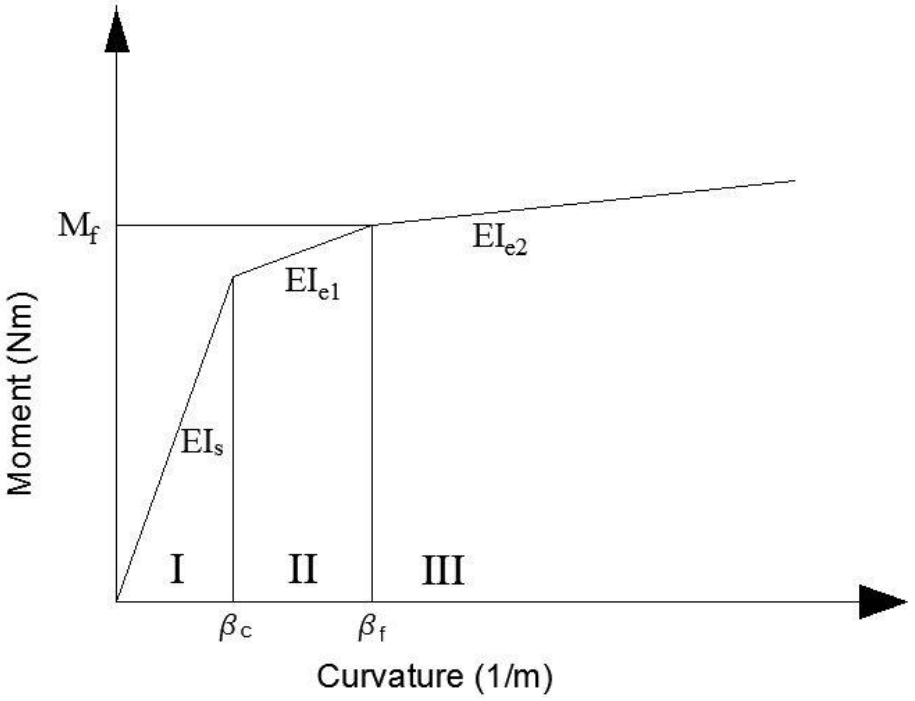

Figure 5 Moment curvature curve

2) Regime II-stick to slip regime

When the curvature exceeds the slip curvature β_c , the internal friction of some wires is smaller than the resulting shear force. Then the pipe enters the stick-to-slip regime (II). In the cross section, wires close to the neutral axis begin to slip relative to each other while the rest

wires are still in the stick regime. The corresponding bending stiffness for this phase is defined as EI_{e1}.

3) Regime III-full slip regime

When all the wires in the cross section start to slip, the pipe enters the full slip regime (III). Each layer and wire is regarded as independent structure. The bending stiffness is the sum of elastic bending stiffness of all plastic layers and metal wires. The moment varies linearly with the curvature in a relative small stiffness EI_{e2}. The corresponding full slip bending moment M_f, depends on the contact pressure between layers which is influenced by the internal and external pressure and the pipe tension.

when the curvature changes its direction, the helical layers attach to each other again and introduce the large internal friction force. The pipe stays in the stick regime again. When the bending moment exceeds twice of the friction moment, the reverse slip occurs. Thereby a hysteresis loop is formed in the moment curvature relationship as shown in Figure 6,.

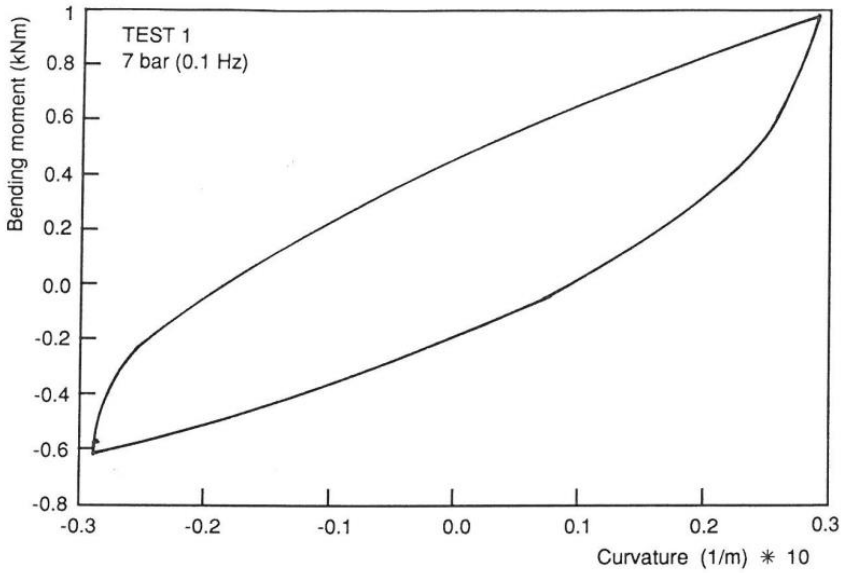

Figure 6 Hysteresis loop[11]

Minimum bend radius

The minimum bend radius is a critical value to prevent excessive bending. Excessive bending can lead to local buckling failure, which particularly occurs during the handling of the pipe. In addition, excessive bending also occurs at the terminations and connections.

The minimum bending radius should consider both the contact radius and the manufacture minimum bending radius. For tensile armour, the minimum bending radius is obtained as

$$\rho_{\min} = \max\left(\frac{R}{1-F_f}, \frac{R}{\delta_{\lim}}\right) \tag{2. 8}$$

$$F_f = \frac{nb}{\cos\alpha 2\pi R} \tag{2. 9}$$

where F_f is the friction filled factor and $\delta_{\lim}$ is the permissible elongation of the outer sheath, which is typically taken as 7.5%.

Bending stress and moments in tensile armour

In order to calculate the bending stress in the tensile armour, the wire is assumed to slip follow a specific curve. The curve is assumed in two ways, as shown in Figure 7:

- The geodesic curve: the shortest distance between two points after bending. Both transverse and longitudinal slips are considered.
- The loxodromic curve: the initial path of wire on the curved plan as if the wire is fixed to the surface. Only consider the longitudinal slip and neglect the transverse slip.

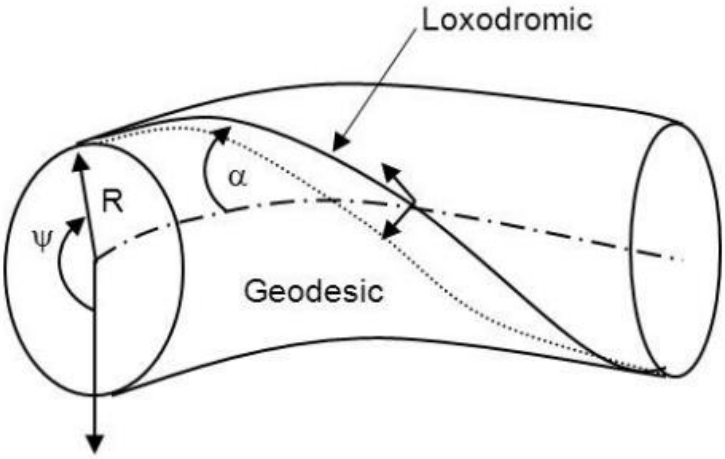

Figure 7 Curvature path [4]

The two important assumptions introduced here are ‘plane section remains plane’ and ‘small deflection’.

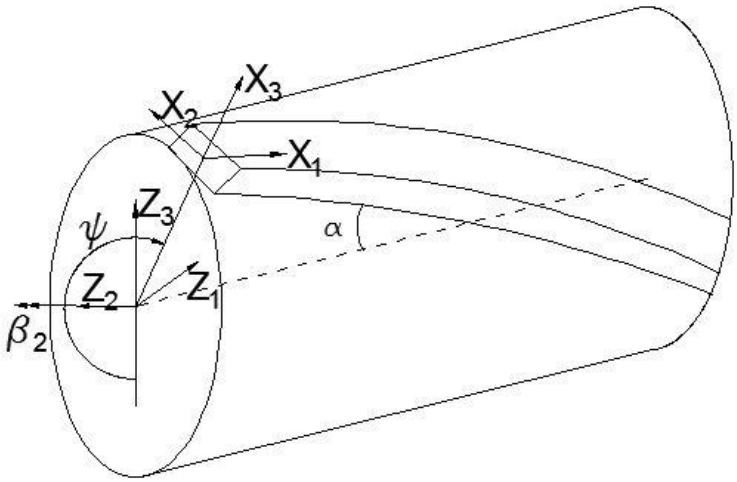

Figure 8 Illustration of tensile armour

Before slip, if only plan deformation is considered, the axial strain and force can be calculated as

$$\varepsilon = -R\cos\psi\beta_2 \tag{2. 10}$$

$$Q_1 = EA\cos\alpha^2\varepsilon \tag{2. 11}$$

$$Q_1 = -EA\cos\alpha^2 R\cos\psi\beta_2 \tag{2. 12}$$

where β_2 is the global curvature at the cross-section center, ψ is the angular coordinate starting from the lowest side of pipe. α is the laying angle of tensile armour, as shown in Figure 8. The shear force per unit length is derived by differentiating the shear force with respect to the length of wire [12]

$$X_1 = \frac{R}{\sin\alpha}\psi \tag{2. 13}$$

$$q_1 = \frac{\partial Q_1}{\partial X_1} = EA\cos^2\alpha\sin\alpha\sin\psi\beta_2 \tag{2. 14}$$

The maximum of shear stress is found at the neutral axis of bending according to the beam theory. Therefore the maximum q_1 corresponds to $\psi = \frac{\pi}{2}$,

$$q_{1,\max} = EA\cos^2\alpha\sin\alpha\beta_2 \tag{2. 15}$$

The shear capacity governed by bending can be described as

$$q_{1c} = \mu(q_3^I + q_3^{I+1}) \tag{2. 16}$$

where μ is the friction coefficient. Pressure from both the inner and outer surfaces should be taken into account. When the shear stress reaches the shear capacity, $q_1 = q_{1c}$, wires at the neutral axis begin to slip relative to each other and the critical curvature is

$$\beta_c = \frac{\mu\left(q_3^I + q_3^{I+1}\right)R}{\sin\alpha A} \tag{2. 17}$$

As shown in Figure 9, when $\beta_2 > \beta_c$, the wires in the cross section can be divided in to stick (I) and slip (II) zones. The angle to divide the two zones can be calculated as

$$\psi_0 = \cos^{-1}(\frac{\beta_c}{\beta_2}) \tag{2. 18}$$

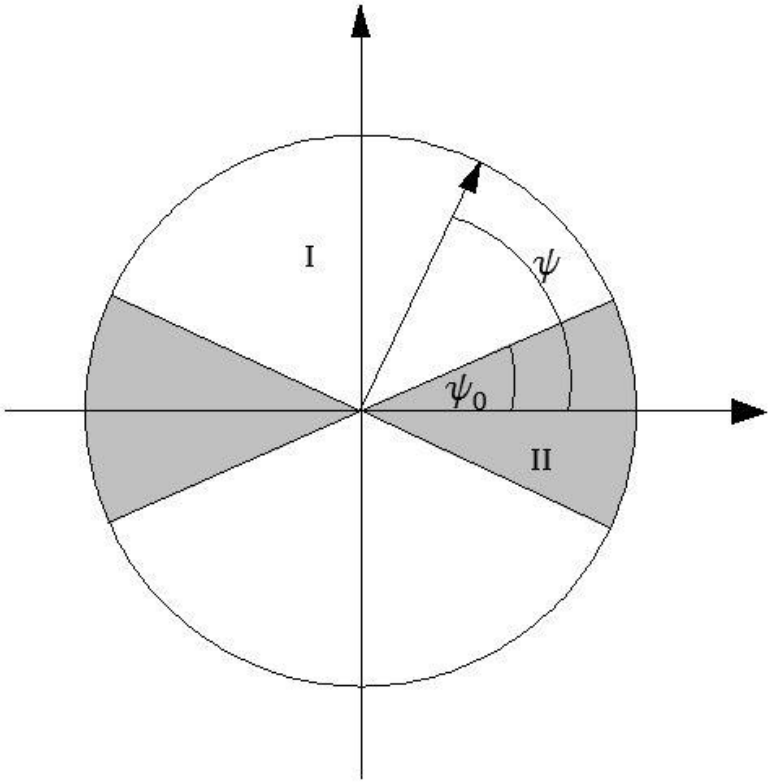

Figure 9 slip zone in cross section

With the curvature and strain relationship, it is possible to calculate the stress distribution in the cross section and the bending moments under curvature β. The stress in Zone I can be expressed as

$$\sigma_{11}(\psi) = E\cos^2\alpha R\beta_2(\sin\psi - \sin\psi_0) + \frac{\mu(q_3^I + q_3^{I+1})R}{\sin\alpha A_t}\psi_0 \qquad (2.\ 19)$$

The stress in Zone II can be expressed as

$$\sigma_{11}(\psi) = \frac{\mu(q_3^I + q_3^{I+1})R}{\sin\alpha A_t}\psi \qquad (2.\ 20)$$

The bending moment could be obtained by integrating the stress along the cross section. When $\psi_0 = 0$, the start slip bending moment is

$$M_c = F_f\,\frac{\pi R^3\cos^2\alpha\mu(q_3^I + q_3^{I+1})}{b\sin\alpha} \qquad (2.\ 21)$$

When ψ_0=90, the full slip bending moment is

$$M_f = F_f \frac{4\pi R^3 \cos^2 \alpha \mu (q_3^I + q_3^{I+1})}{b \sin \alpha} \tag{2. 22}$$

The total bending stiffness contains two parts: (1) elastic bending from the plastic layers and local wire bending; (2) the structure bending from friction between layers.

$$EI = EI_e + \sum_{i=1}^{N_t} F_{fi} \cos^4 \alpha_i \pi R_i^3 t_i f\left(\beta_2, \beta_{ci}\right) \tag{2. 23}$$

where f is a function that is zero when $\beta > \beta_c$ for each layers. Therefore after slip starts, the structural bending has no contributions to total stiffness anymore. Elastic bending plays the dominate role in bending stiffness.[13] [14]

2.2.3 Damping

There are many sources of damping related to the global response of riser, including viscous damping and structural damping. This thesis focuses on the influence of hysteresis damping on the structure. Hyesteresis damping is mainly due to the internal friction and sliding in the material. The energy loss due to damping can be described by the area within the hysteresis loop.

Linearization of hysteresis damping in flexible pipes

As discussed in the bending property of the flexible pipe, the moment curvature relationship for the flexible pipe is nonlinear due to internal friction and slip behavior. The loop formed in the curve represents the energy consumed by hysteresis damping.

By assuming an equivalent linear viscous damping coefficient c_{eq}, the damping moment is proportional to the curvature gradient $\dot{\kappa}$ as

$$M_d = c_{eq} \dot{\kappa} \tag{2. 24}$$

where $\kappa = \kappa_0 \cos(\omega t)$. The work done by linear damping moment can be calculated as

$$W_d = 4\int_L \int_0^{\frac{T}{4}} c\kappa_0 \cos(\omega t) c\kappa_0 \cos(\omega t) dt dx = \pi c \kappa_0^2 \omega \tag{2. 25}$$

Assume the real energy dissipation per cycles equals to the linearized damping energy loss, then

$$c_{eq} = \frac{W_0}{\pi \kappa_0^2 \omega} \tag{2. 26}$$

W_0 can be calculated as the area of hysteresis loop in the moment curvature curve.

Then the nonlinear hysteresis damping could be linearized as an equivalent linear viscous damping.

2.2.4 Fatigue

Fatigue damage is a progressive and localized structure damage that occurs when the structure is subjected to cyclic loading. Flexible risers in waves may experience the following motions that could lead to fatigue damage[15]:

- first order response to waves
- second order floater motions
- vortex induced vibration
- installation and transportation

The fatigue life of a material includes the crack initiation phase and crack propagation phase. For an un-welded component, the crack initiation phase takes over 95% of the total fatigue life.

The long term fatigue life analysis of dynamic flexible riser is performed by the following procedure:

- Subdivide the wave environment scatter diagram into a number of representative blocks. A single sea state is selected to represent all the sea states within the block.
- Conduct global analysis of the flexible riser in each sea state to obtain history series of tension, curvatures and moments.
- Transform the global quantities into a local model and conduct the fatigue damage computation.
- Calculate the weighted fatigue damage accumulation from all sea states based on the Miner-Palmgren rule

$$D = \sum_{i=1}^{k} \frac{P_i n_i}{N_i} \tag{2. 27}$$

where P_i represents the sea states probability, n_i represents the number of stress cycles that occurs within a certain period, N_i represents number of stress cycles to failure according to the S-N curve of the material and k represents number of discrete sea states of the scatter diagram.

The basic fatigue capacity is given by the S-N curve which expresses the number of stress cycles to failure, N for a given constant stress range, S[16]:

$$N_i = aS^{-m} \tag{2. 28}$$

where a and m are constants obtained by fatigue testing. The typical S-N curve of steel material in air environment is shown in Figure 10.

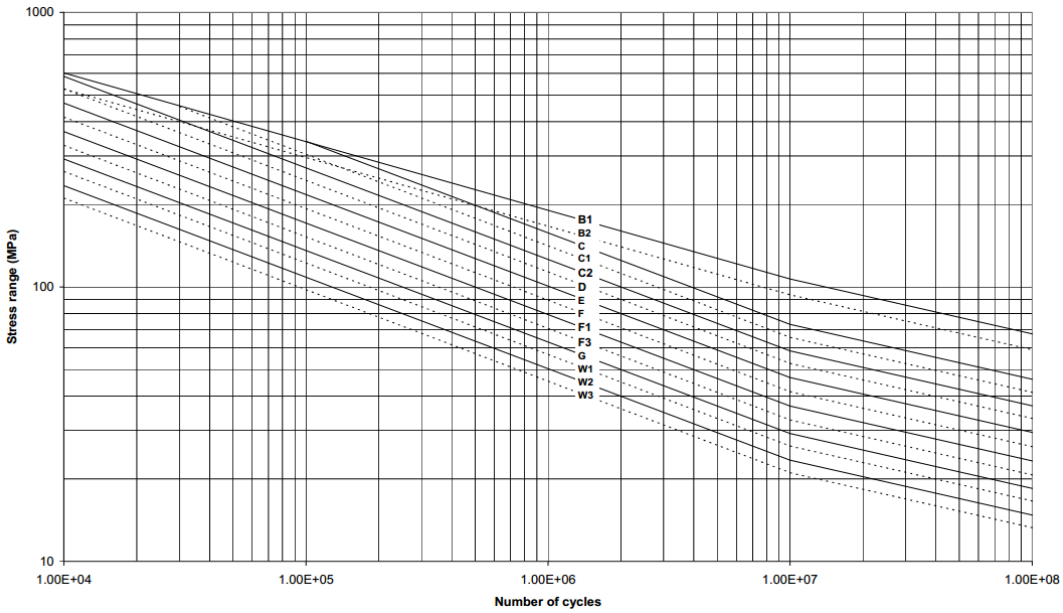

Figure 10 S-N curve in air [16]

2.3 Flexible pipe design

Flexible pipes will experience dynamic loads from waves and the motion of vessels. The cyclic bending moment imposed on the riser will cause fatigue damage of the pipes.[17] The design of flexible pipe is conducted based on the following codes:

ISO 13628-2, equivalent to API spec 17J[2] (Non-bonded flexible pipe)

ISO 13628-11, equivalent to API RP 17B[1] (Recommended practice for flexible pipe)

DNV-RP-F204, Recommended practice for riser damage

DNV-RP-D101, Recommended practice for structural analysis of piping systems

The following design considerations are based on code API RP 17B[3].

2.3.1 Failure modes of pipe design

The failure modes of the riser are essential to the pipeline design. A checklist of failure modes for primary structural design of unbonded flexible pipe and the corresponding design solutions is give in Table 1.

Table 1 Checklist of failure modes for primary structural design of unbonded flexible pipe[3]

Failure mode	**Potential failure mechanisms**
Collapse	Collapse of carcass and/or pressure armour due to excessive tension, excessive external pressure, installation loads or ovalisation due to installation loads. Collapse of internal pressure sheath in smooth bore pipe. Collapse of carcass due to pressure build up in multilayer pressure sheaths followed by rapid decompression. Collapses of pipe due to carcass pull out from end fitting. Collapse of carcass due to the carcass fatigue.
Burst	Rupture of pressure armours because of excess internal pressure. Rupture of tensile armours due to excess internal pressure.
Tensile failure	Rupture of tensile armours due to excess tension. Snagging by fishing trawl board or anchor, causing overbending or tensile failure.
Compressive failure	Birdcaging or lateral buckling of tensile armour wires. Compression leading to upheaval buckling and excess bending.
Overbending	Collapse of carcass and/or pressure armour or internal pressure sheath. Rupture of internal pressure sheath. Unlocking of interlocked pressure or tensile armour layer. Crack in outer sheath.
Torsional failure	Failure of tensile armour wires Collapse of carcass and/or internal pressure sheath. Birdcaging of tensile armour wires.
Fatigue failure	Tensile armour wire fatigue. Pressure armour wire fatigue.
Erosion	Erosion of internal carcass.
Corrosion	Corrosion of internal carcass. Corrosion of pressure or tensile armour exposed to sea water. Corrosion of pressure or tensile armour exposed to diffused product.

It is noted that one failure modes may induce the other failure modes. In addition, the excessive internal pressure, external pressure, tension and compression forces are the main issues that will lead to pipe failure.

2.3.2 Flexible pipe design criteria

The design criteria of flexible pipe should be satisfied to avoid the failures. Design criteria are defined by the limiting stress divided by the structural capacity. The structural capacity utilizes either the yielding stress or 0.9 times the ultimate tensile stress of the currently used material. The Code API SPEC 17J specifies the following design criteria.

Strain

The allowable strain is defined for the design of the internal pressure sheath and outer sheath. The criterion of maximum allowable strain is 7.7% for PE and PA, 7.0% for PVDF in static applications and for storage in dynamic applications. For dynamic operation, the limiting value is 3.5% for PVDF.

Creeping

Creep means the internal pressure sheath deforms into the gaps of tensile armour or pressure armour due to pressure or temperature effect. Therefore the thickness of the internal pressure sheath should be limited so that collapse will not occur even if the layer gets thinner. The maximum allowable reduction in layer thickness is 30% under all load combinations.

Stress

The design criteria for stress specify the ratio between the maximum allowable average layer stress and the structural capacity of the steel. The allowable factor varies between designing conditions. For example, the design criterion for tensile armour under the functional and environmental loads in normal operation is 0.67. If taking the accidental load into consideration, the allowable factor is 0.85.

Hydrostatic collapse

To avoid collapse of internal carcass due to hydrostatic pressure, the utilization factor is defined by dividing the differential pressure by the hydrostatic pressure. The differential pressure is calculated as the external hydrostatic pressure minus the local internal pressure.

Mechanical collapse

Mechanical collapse is induced by the excessive stress from armour layers. It should be noted that the stress components from all the supporting steel layers should be taken into consideration.

Torsion

During installation and service conditions, the pipe will experience torsional moment. The torsional stiffness of the flexible pipe should be strong enough to resist this torsional load.

Crushing collapse and ovalisation

When the pipe is laid down, it is reeled in a sheave and strengthened by a tensioner. The tension force in the pipe should be well design otherwise a sudden collapse might occur due to excessive radical compression. Both the radical compression loads and maximum axial loads should be checked to satisfy the design criteria.

Compression

Excessive compression in flexible pipes should always be avoided since it will lead to instability, overbending, birdcaging and lateral buckling. The allowable compression is determined by the design criteria in API spec 17J, the allowable value given by the manufacture and the pipe minimum bending radius criterion.[18]

Service life factor

The fatigue lifetime prediction is based on the material properties given by testing, such as the S-N curve. The API spec 17J specifies the detailed criterion for lifetime analysis.

3 Nonlinear Finite Element Method

Finite element method is a numerical procedure for analyzing structures and continua. It can deal with models with arbitrary shape, loads and support conditions. In finite element model, the system is discreted into small pieces and the equilibrium is established in the element level. Due to the high nonlinearity in the flexible riser configuration, material property and loading conditions, nonlinear finite element method is applied for analysis.

In this chapter, the nonlinearities in the analysis of flexible pipes will be discussed; the general principle and key formulations of the finite element method will be reviewed. Besides, introduction to the nonlinear finite element code BFLEX and SIMLA will also be presented.

3.1 Nonlinearity in flexible pipe analysis

Flexible pipe has the characteristics of low bending stiffness, large deformation and layered structure. Therefore the analysis of the flexible pipes is of high nonlinearities. The most dominate nonlinear effects are

- Large displacement: the flexible pipe will experience very large deformation and displacement when it is laid down from the vessel.
- Nonlinear material behavior: the material become plastic when the strain exceeds the proportional limit therefore the elastic-plastic material model should be adopted.
- Nonlinear hydrodynamic loading: under waves and currents, the hydrodynamic loads are proportional to the square of the relative velocity according to the Morsion equation.

- Nonlinear pipe-soil interaction forces
- variable boundary conditions
- Transient temperature and pressure loads

In order to simulate the above nonlinear effects, a nonlinear finite element analysis is required. The thesis is based on the nonlinear finite element code BFLEX and SIMLA which has been extensively developed to conduct pipeline design and analysis.

3.2 Nonlinear finite element formulations

The following formulations are based on the Theory manual of SIMLA[19].

3.2.1 Principle of virtual displacement

The principle of virtual displacement is utilized to setup the total equilibrium. The principle is applied by assuming a kinematically admissible displacement to the system, and then the total work performed by the system is in equilibrium, in another word, the external virtual work equals the internal virtual work. The principle of virtual work in an arbitrary equilibrium is[19]

$$\int_V (\rho \ddot{\mathbf{u}} - \mathbf{f}) \delta \mathbf{u} \delta V + \int_V (\boldsymbol{\sigma} - \boldsymbol{\sigma}_0) \delta \varepsilon \delta V - \int_S \mathbf{t} \delta \mathbf{u} \delta S = 0 \qquad (3.1)$$

where ρ is the material density, $\mathbf{u}$ is the displacement vector, $\mathbf{f}$ is the volume force vector, $\boldsymbol{\sigma}$ is the stress tensor of Cauchy stress, $\boldsymbol{\sigma}_0$ is the stress tensor of initial stress, ε is the natural strain, $\mathbf{t}$ is the surface traction.

The first term in the equation is related to the inertial force. The second term is the work done by the internal forces and the last term is the work done by the external forces at the assumed virtual displacement.

Total Lagrangian and Updated Lagrangian methods are the two basic formulations. In a Total Lagrangian formulation, all static and kinematic variables are referred back to the initial

conditions. In the Updated Lagrangian incremental form, variables are calculated based on the last obtained configuration. In BFLEX and SIMLA, the Corotated Total Lagrangian formulation is used which means the element reference system is fixed to the element but its position and orientation is updated at each load step.

In order to develop finite element equations, the following formulations are needed[19, 20]:

- A kinematic relationship between the displacements, rotations and strains at a material point.
- A material law connecting the strain with resulting stress.
- Displacement interpolation.

In the finite element analysis, variables are calculated by the incremental methods and the interactive methods. The incremental equation for the stiffness matrix is expressed as

$$\int_V \mathbf{C} : \Delta\mathbf{E} : \delta\mathbf{E} dV_0 + \int_V \boldsymbol{\sigma} : \Delta\mathbf{E} dV_0 - \int_S \Delta\mathbf{t} dS_0 = 0 \tag{3. 2}$$

wehre **C** represents the tangential material stiffness, **E** represents the Green strain tensor. The first term gives the material stiffness matrix and second term gives the geometric stiffness matrix.

3.2.2 Kinematic relationship

The kinematic relationship refers to the relationship between displacements and strain. Based on the Euler-Bernoulli beam theory, for an arbitrary point P in the cross section, the displacement **u** can be described by axial elongation, torsion and bending as

$$\mathbf{u} = u_1\mathbf{G_1} + u_2\mathbf{G_2} + u_3\mathbf{G_3} \tag{3. 3}$$

$$u_1 = u_1^0(X^1) + X^3\theta_2(X^1) - X^2\theta_3(X^1) + \beta(X^1)\varphi(X^2, X^3) \tag{3. 4}$$

$$u_2 = u_2^0(X_1) - X^3\theta_1(X^1) \tag{3. 5}$$

$$u_3 = u_3^0(X_1) + X^2\theta_1(X^1) \tag{3. 6}$$

where u_i is the displacement component with the unit vector $\mathbf{G_i}$, u_i^0 is the displacement along the centerline X^i and θ_i is the rotation with respect to axes i. $\varphi(X^2, X^3)$ is the warping equation of Saint-Venant's torsion. β is initially assumed to be an arbitrary function of X^i. The coordinate system is shown in Figure 11.

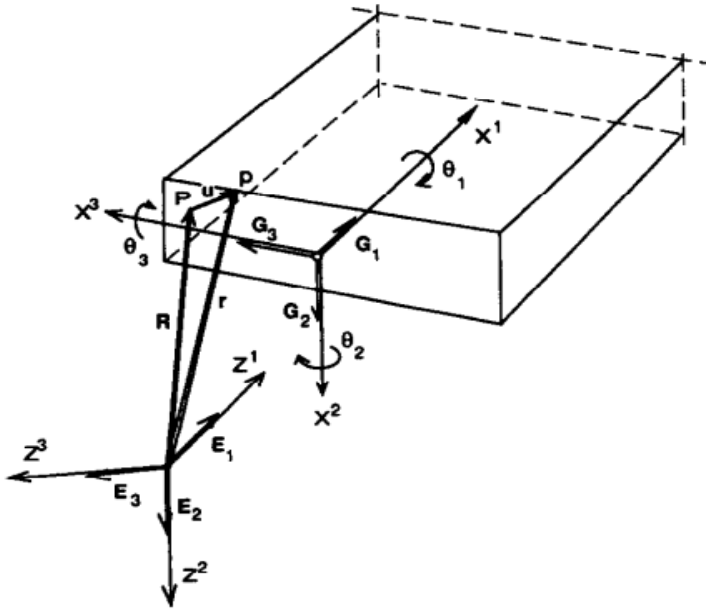

Figure 11 Coordinate system[19]

Assume the initial position vector of point P is **R**, the position after deformation is described as

$$\mathbf{r} = \mathbf{R} + \mathbf{u} \tag{3. 7}$$

By based on the displacement vector, the green strain can be obtained as

$$GE_{11} = \varepsilon_1 + X^3\omega_2 - X^2\omega_3 + \varphi\beta_{,1} + \kappa_1\beta\left[X^3\varphi_{,2} - X^2\varphi_{,3}\right] + \frac{1}{2}\varepsilon_1^2 + \frac{1}{2}\varepsilon_2^2 + \frac{1}{2}\varepsilon_2^2 \tag{3. 8}$$

$$2\sqrt{G}E_{12} = \varepsilon_2 - \theta_3 - X^3\omega_1 + \beta\left[\sqrt{G}\varphi_{,2} + \kappa_3\varphi\right] \tag{3. 9}$$

$$2\sqrt{G}E_{13} = \varepsilon_3 + \theta_2 + X^2\omega_1 + \beta\left[\sqrt{G}\varphi_{,3} - \kappa_2\varphi\right] \tag{3. 10}$$

where the ',i' indicates the differentiation with respect to the axis i and

$$\varepsilon_1 = u_{1,1}^0 - \kappa_3 u_2^0 + \kappa_2 u_3^0 \tag{3. 11}$$

$$\varepsilon_2 = u^0_{2,1} + \kappa_3 u^0_1 - \kappa_1 u^0_3 \quad (3.12)$$

$$\varepsilon_3 = u^0_{3,1} - \kappa_2 u^0_1 + \kappa_1 u^0_2 \quad (3.13)$$

$$\omega_1 = \theta_{1,1} - \kappa_3 \theta_2 + \kappa_2 \theta_3 \quad (3.14)$$

$$\omega_2 = \theta_{2,1} + \kappa_3 \theta_1 - \kappa_1 \theta_3 \quad (3.15)$$

$$\omega_3 = \theta_{3,1} - \kappa_2 \theta_1 + \kappa_2 \theta_2 \quad (3.16)$$

where κ_1 corresponds to the torsional curvature and κ_2 , κ_3 are the bending curvature with respect to xz and xy plane. G is a parameter determined as

$$G = (1 + X^3 \kappa_2 - X^2 \kappa_3)^2 \quad (3.17)$$

So far the relationship between the strain and displacement has been established. [8, 21]

3.2.3 Material law

The material law means the relationship between the stress and strain of the material. For example, if the material is elastic, then the stress varies linearly with the strain by means of Hooks's law. If the material is elastoplastic, the plastic strains will occur if the stress exceeds the yielding stress which leads to a nonlinear stress strain curve.

In this thesis, the element PIPE52 is adopted which represents an elastic material and account for the both the asymmetric loads bending moments. The relationship between stress and strain under tension, torsion and bending moment has been discussed in section 0,0 and 2.2.2. [22]

3.2.4 Displacement interpolation

The displacement within the element is interpolated from the displacements of the boundary nodes. The shape function **N** is introduced to define how the displacement varies within the element.

Beam element is described by 12 dofs, as shown in Figure 12. For beam element, linear interpolation is used for the torsional rotation $\mathbf{u}_\theta$ and the axial displacement $\mathbf{u}_x$ and cubic interpolation is used in the transverse displacement $\mathbf{u}_y$ and $\mathbf{u}_z$

$$\begin{aligned} u_{x0} &= \mathbf{N}_x \mathbf{u}_x \\ u_{y0} &= \mathbf{N}_y \mathbf{u}_y \\ u_{z0} &= \mathbf{N}_z \mathbf{u}_z \\ u_{\theta 0} &= \mathbf{N}_\theta \mathbf{u}_\theta \end{aligned} \tag{3. 18}$$

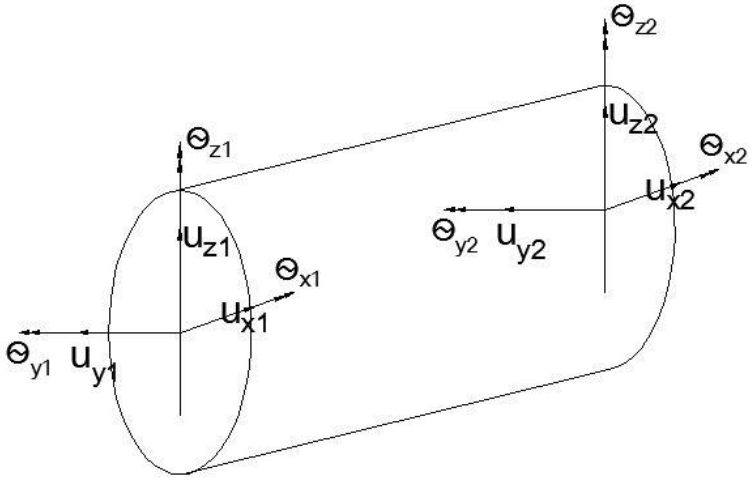

Figure 12 Dofs for PIPE element

For concrete coating element, such as the element for tendon displacement, four local longitudinal dofs $\mathbf{v}_s$ are added to describe the shear interaction, as shown in Figure 13. Therefore in addition equation (3.17), $v_{s,0} = \mathbf{N}_s \mathbf{v}_s$ is also included in the interpolation function.

$\mathbf{N}_s$ is described as a cubic polynomial function.

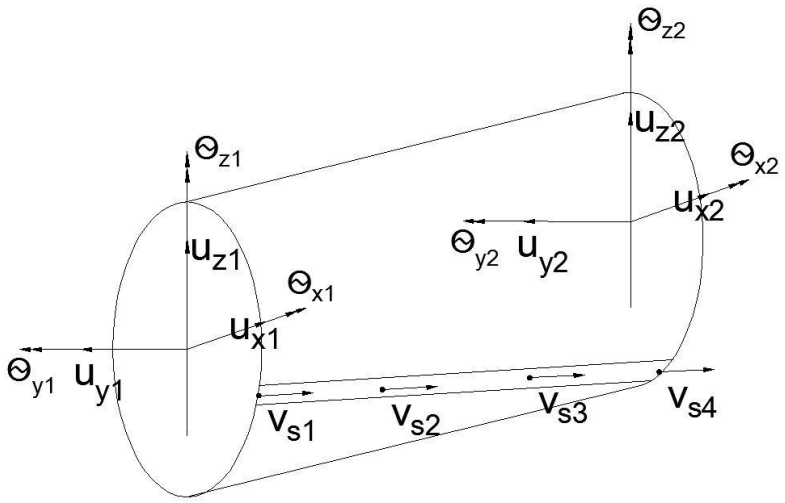

Figure 13 Dofs for concrete coating element

3.3 Solution algorithms

3.3.1 Static solution procedure

Static solution procedure is conducted by increment of user defined load step with Newton-Raphson equilibrium interaction at each step. The procedure is

$$\Delta r_{k+1}^{i} = K_{T,k+1}^{-i} \Delta R_{k+1}^{i} \tag{3. 19}$$

where ΔR_{k+1}^{i} is the load increment from load step k to k+1. The increment in load leads to the displacement increment Δr_{k+1}^{i}. The stiffness matrix K is updated for each step. The interactions are repeated until convergence is obtained.

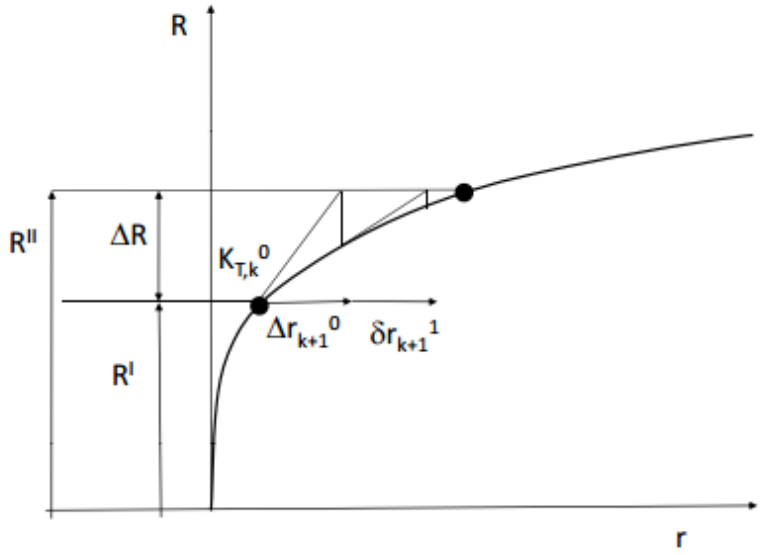

Figure 14 Illustration of Newton Raphson integration[23]

3.3.2 Dynamic solution procedure

For nonlinear dynamic problem, the direct time integration of the motion is necessary. There are explicit and implicit methods to conduct the integration. For explicit methods, the displacement at time step k+1 depends on the displacement at time k and k-1. It is a conditional stable method and requires very small steps. Therefore it is widely used in the analysis of explosion and impact problems. For implicit methods, the displacement at time step k+1 depends on the displacement information at time k+1 and time k. Since the implicit method depends on the time step k+1, it is more stable than the implicit method.

For the implicit method, there are different ways to define the acceleration between the two time steps

$$\ddot{u} = f(\ddot{u}_{k+1}, \ddot{u}_k) \tag{3. 20}$$

- Average acceleration

$$\begin{aligned} \ddot{u} &= \frac{1}{2}\left(\ddot{u}_k + \ddot{u}_{k+1}\right) \\ \dot{u} &= \dot{u}_k + \frac{1}{2}\left(\ddot{u}_k + \ddot{u}_{k+1}\right)\Delta t \end{aligned} \tag{3. 21}$$

Together with the dynamic equilibrium equation, we have three equations and three unknowns, it is sufficient to solve the unknowns. This method is unconditionally stable.

- Newmark β integration

$$\begin{aligned} \dot{u}_{k+1} &= \dot{u}_k + (1-\delta)\ddot{u}_k \Delta t + \delta \ddot{u}_{k+1} \Delta t \\ u_{k+1} &= u_k + \dot{u}_k \Delta t + (\frac{1}{2} - \beta)\ddot{u}_k \Delta t^2 + \beta \ddot{u}_{k+1} \Delta t^2 \end{aligned} \tag{3. 22}$$

where δ and β are the weight factors for velocity and displacement from accelerations at k and k+1. They are determined by the requirements related to stability and accuracy. Then $\dot{u}_{k+1}, u_{k+1}$ can be expressed by $\ddot{u}_{k+1}$. Together with

$$M\ddot{u}_{k+1} + C\dot{u}_{k+1} + Ku_{k+1} = \mathrm{R}_{k+1} \tag{3. 23}$$

$\ddot{u}_{k+1}$ can be solved and then all the quantities in time k+1 become known. The solution is stable if

$$\delta \geq \frac{1}{2}$$

$$\beta \geq \frac{\left(\delta + \frac{1}{2}\right)^2}{4} \tag{3. 24}$$

In the dynamic analysis, we are more interested in the low frequency modes. To calculate the high frequency modes consume a large numerical effort. Therefore it is common to damp out these high order modes and describe the lower order modes with better accuracy. Numerical damping and Rayleigh damping can be introduced in Nermark β method to damp out the medium modes. The HHT-α method can damp out the higher order frequency and at the same time retain 2nd order accuracy.

The equilibrium of equation (3.19) is assumed to be achieved if the following tolerance level is satisfied

$$\left\|\delta \mathbf{r}_{k+1}^{i+1}\right\| < \varepsilon_d \left\|\mathbf{r}_{k+1}^{i+1}\right\| \tag{3. 25}$$

$$\left\|\mathbf{r}_{k+1}^{i+1}\right\| = \frac{1}{N}\sqrt{\sum_{j=1}^{N}\left(r_j^{i+1}\right)^2} \tag{3. 26}$$

$$\left\|\delta \mathbf{r}_{k+1}^{i+1}\right\| = \left\|\mathbf{r}_{k+1}^{i+1}\right\| - \left\|\mathbf{r}_{k+1}^{i}\right\| \tag{3. 27}$$

where ε_d is the tolerance criteria which is usually in the order 10^{-5} to 10^{-7}. After the equilibrium is achieved, a new load increment ΔR will be given to the system.

3.4 Nonlinear finite element code

The local analysis and global analysis of flexible pipe in this thesis are based on the nonlinear finite element code BFLEX and SIMLA respectively.

3.4.1 BFLEX application

BFLEX[22] is a finite element program especially designed to conduct the service life analysis of deep water riser by SINTEF. BFLEX contains modules: BFLEX2010, PFLEX, BOUNDARY AND LIFETIME.

BFLEX2010 module reads and control the input data and can perform the global and tensile armour analysis.

BFLEX2010POST module generates the result files that can be further analyzed in other module. PFLEX and BOUNDARY conducts the beam and transverse stress analysis of the pressure spirals.

LIFETIME performs fatigue calculations and post processing.

XPOST can be used for graphical visualization.

The mechanical theory on flexible pipe in BFLEX is based on the work of Svein Sævik [2] [8]. The axisymmetric strains and bending strains are assumed to be uncoupled. There are three bending formulations to simulate the bending behavior of tensile armour.

ITCODE0 considers the shear stress between each individual tendon and the pipe core.

ITCODE21 considers the friction moment contributions from all layers but use one moment curvature relationship to represent all the layers.

ITCODE31 considers the friction moment contribution from all layers and create a moment curvature curve for each layer. Therefore the slip behaviors of all the layers are involved.

In BFLEX, the transverse displacement of tendon is neglected and the tendon is assumed to slide only in the longitudinal direction, i.e. the loxodromic curve is assumed.

3.4.2 SIMLA application

SIMLA[23] is the software developed for the analysis of offshore pipelines in deep waters and rough environments. SIMLA can realize the functions of nonlinear 3D FEM static and dynamic analysis, simulation of pipe laying, evaluation of laying stability, upheaval buckling and snaking analysis, inspection and evaluation of free spans and route planning and optimization. In this thesis, SIMLA is going to be utilized to conduct the global response analysis of flexible riser. Typically the analysis procedure is established as following:

1) Static analysis is used in the first phase to establish the initial configuration and then dynamic analysis follows the current step. This is realized by the command CONTROL and use RESTART. TIMECO card can control the step length and type of analysis.
2) It should be noted that the result file of the static analysis is the input file for the dynamic analysis if we use RESTART command. Usually definition on the interval of storage is important since otherwise the result file will be very large. Therefore VISRES card should be activated.
3) Define the nodes and elements and their properties.

4) Define the materials properties.

5) Define the boundary conditions, loading conditions and constraints. Time histories can be defined to control the loading patterns during simulation.

6) To simulate the response of riser in waves, wave data and RAO data are included in the analysis.

7) Visualize the results in XPOST.

8) Generate results with SimPost.

By defining different material types, linear damping model and nonlinear damping model can be setup in the model.

4 Influence of Hysteresis Effect in Bending Mode

Flexible pipe response is governed by significant hysteresis in the bending mode. Hysteresis damping can be explained as: under a large bending curvature, pipe layers slide relative to each other; the internal friction force between layers lead to energy loss which affect the global response of the riser. In order to study the influence of this effect, it is preliminary to identify the behaviour of the flexible pipes under cyclic bending moment.

The work will be carried out as follows:

- Conduct local analysis to establish the cross sectional properties of flexible pipe.
- Perform global analysis to obtain the global curvature and moment responses of the flexible riser.
- Study the bending behaviors of the pipes along the riser.

If the results prove that the slip behavior occurs in a wide range of the riser under wave loads, then a linear viscous damping model will be established to investigate the influence of the nonlinear damping effects in flexible risers.

4.1 Local analysis

The purpose of the local analysis of a flexible pipe is to investigate the cross sectional mechanical properties of the pipe. In this section, the axial stiffness, torsional stiffness and bending properties of the pipe are presented.

4.1.1 Modeling of pipe cross section

Model property

The model for the local analysis is a flexible pipe with steel and plastic layers. The steel layers include carcass, pressure spirals and tensile armours. The plastic layers include antiwear layers, barriers and protective sheath. The general pipe properties are given in Table 2. The pipe model is shown in Figure 15. More detailed properties and dimensions of the pipe layers are available in Appendix A.

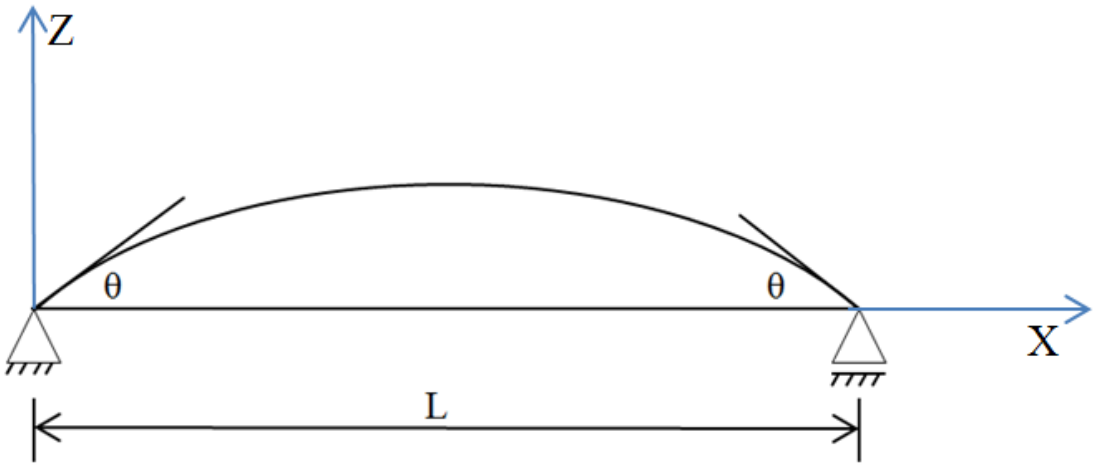

Figure 15 Pipe model

Table 2 Properties of the pipe

Property	Units	Value
Internal diameter	mm	228.6
External diameter	mm	401.0
Internal pressure	MPa	47.5
Length of model	mm	100

The modeled pipe length is very short. The consideration is that for the pipe of short length, the bending radius along the pipe can be assumed to be uniform if a prescribed rotation is applied at the ends. The curvature can be calculated as

$$\kappa = \frac{2\theta}{L} \tag{4. 1}$$

where L is the length of the pipe and θ is the prescribed rotation at ends. It should be noted that the prescribed curvature should be larger than the critical curvature so that the slip

behavior could initiate between the layers. In addition, the curvature should be smaller than the value that corresponds to the minimum bending radius, otherwise failure might occur.

Mesh

There are 11 nodes uniformly distributed along the pipe. Pipe 52 element is adopted since it is a three dimensional moment based element. The mesh result is shown as Figure 16.

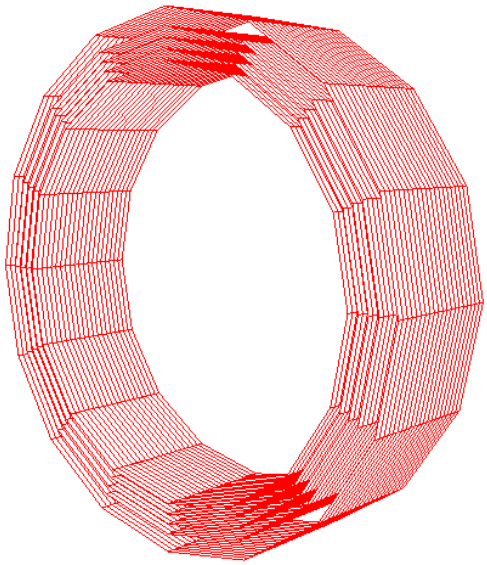

Figure 16 Mesh of pipe in BFLEX

Boundary and loading

The boundary of pipe is shown as Figure 15 . The left end is simply supported and the right end is restrained to move in y and z direction but free to move along x axis.

The internal pressure is 47.5 MPa. The tension force of 935093 N is applied at the right end.

The bending and torsional properties are studied by prescribing rotations at the ends. The axial stiffness is examined by introducing a forced displacement along pipe axis.

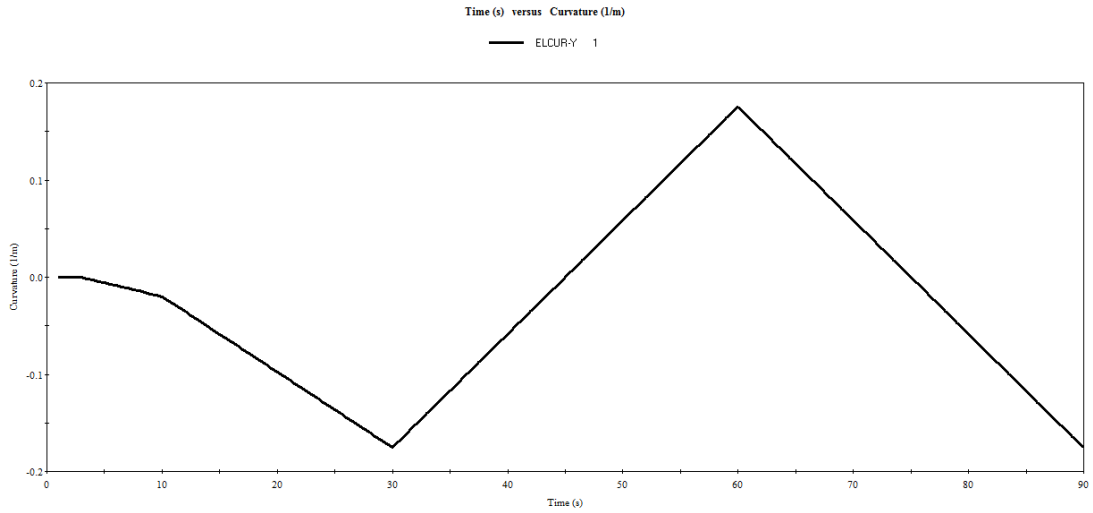

Figure 17 Time series of curvature

4.1.2 Cross sectional characteristics

Moment-curvature characteristics

To investigate the bending property, a time varying prescribed rotation is introduced to the 5th dof of both ends to cause the bending moment. The magnitude of rotation is 0.00875 rad. The resulting curvature variation is shown in Figure 17. It should be noted that the increment step for curvature around the slip curvature β_c should be small enough in order to capture the transition of the pipe layers from stick to slip correctly.

The axial stress distribution is shown as Figure 18. Due to the bending effects, axial stress is higher in the upper part than in the lower part. In addition, the inner layer has larger bending stress than the outer layer. This can be explained that the axial stress σ_{11} is proportional to the friction coefficient multiplying by the pressure load, explained by equation (2.19) (2.20). Since the pressure load in the inner layer is larger than the outer layer, the axial stress of inner layer will be higher.

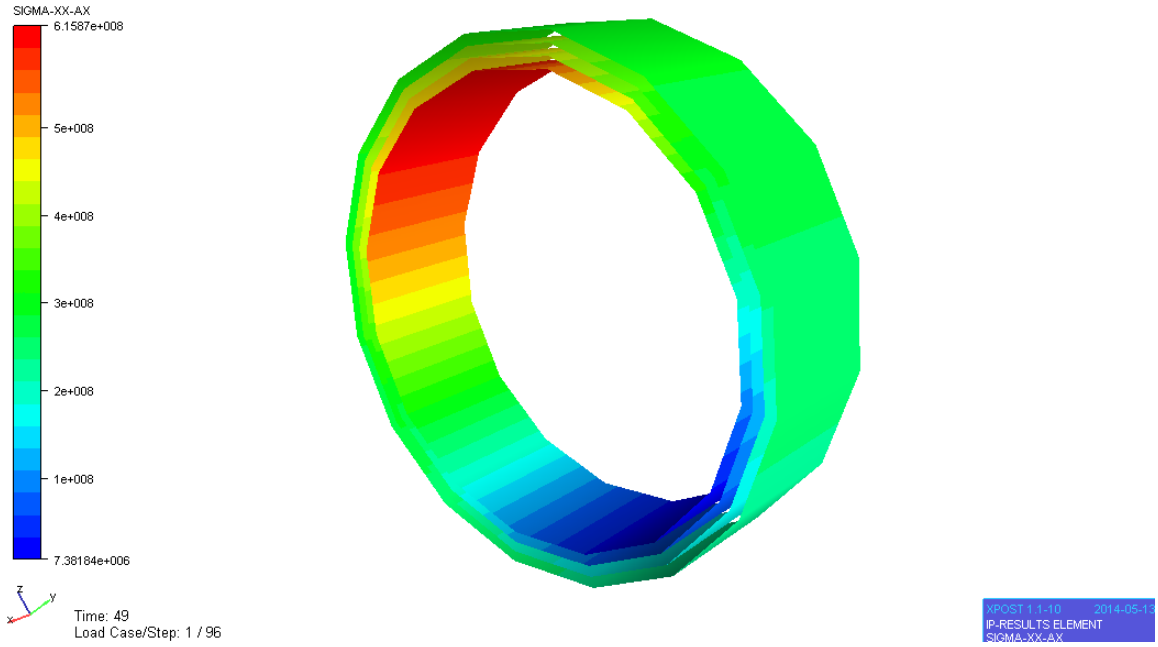

Figure 18 Stress distribution of pipe model

The moment curvature relationship is obtained by adding up the moment contributions from each layer. A hysteresis loop is formed in the moment curvature curve, as shown in Figure 19. When the pipe starts to bend, the shear force between layers in less than the internal friction and the pipe is in the stick phase. The bending stiffness is $EI_S = 8.8E6$ Nm^2. When the curvature of the pipe is over the slip curvature $\beta_c = 0.013$, the wires in the pipe layers start to slip. Then the bending stiffness reduces to $EI_{e1} = 9.6E5$ Nm^2. When the resulting bending moment exceeds the fiction moment M_f =131084 Nm, all the wires in the tensile armour start to slip relative to the other layers. The moment varies linearly with curvature with the elastic bending stiffness $EI_{e2} = 3.5E5$ Nm^2. As the direction of curvature changes, the change in moment has to exceed twice of the friction moment before reverse slip behavior occurs. The moment curvature curves form a hysteresis loop. The area of the loop is 84000N which corresponds to the energy loss per meter due to hysteresis damping.

Axial force-strain characteristics

The axial stiffness is measured by applying a forced displacement x=0.005 at the end node. The axial force varies linearly with the strain as shown in Figure 20. By linear fitting, the axial stiffness is obtained as $EA = 3E9$ N.

Torque-torsion characteristics

A forced rotation is introduced to the 4th dof of the end nodes. The torque and torsion is in a linear relationship, shown in Figure 21. The torsional stiffness is $GI_t = 3.4E7$ Nm/rad.

The the key parameters of cross sectional characteristics are summarized in Table 3.

Table 3 bending stiffness parameter

Parameter	Value
EA (N)	3E9
GI_t (Nm/rad)	3.4E7
EI_s (Nm^2)	8.8E6
EI_{e1} (Nm^2)	9.6E5
EI_{e2} (Nm^2)	3.5E5
β_c (m^{-1})	0.012
β_f (m^{-1})	0.031

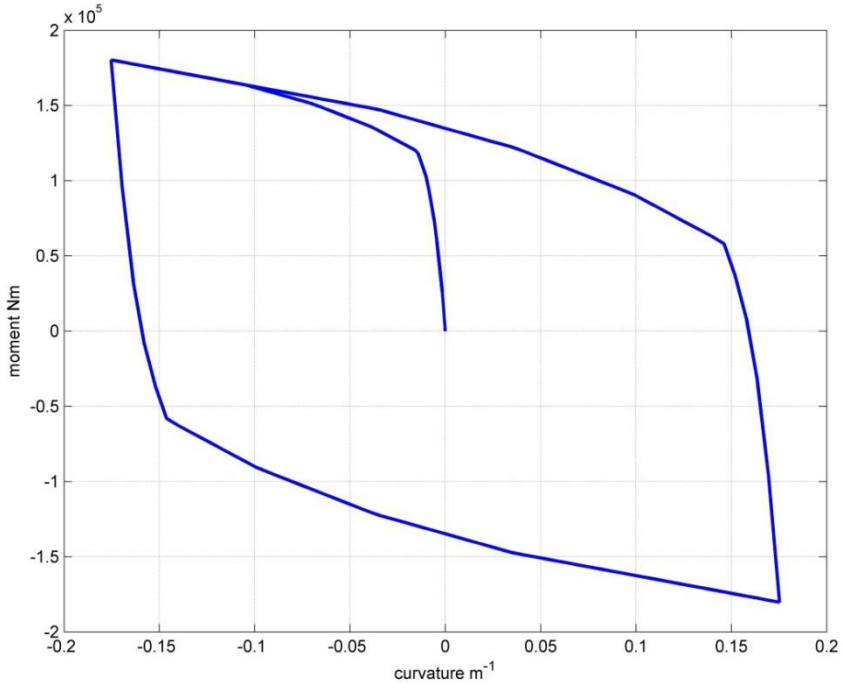

Figure 19 Moment curvature relationship

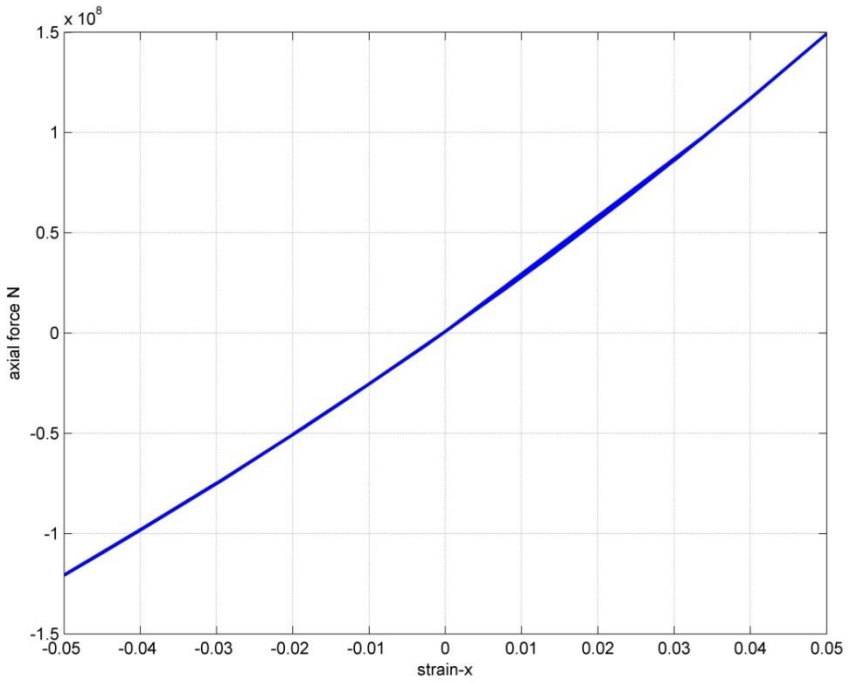

Figure 20 Axial force and strain relationship

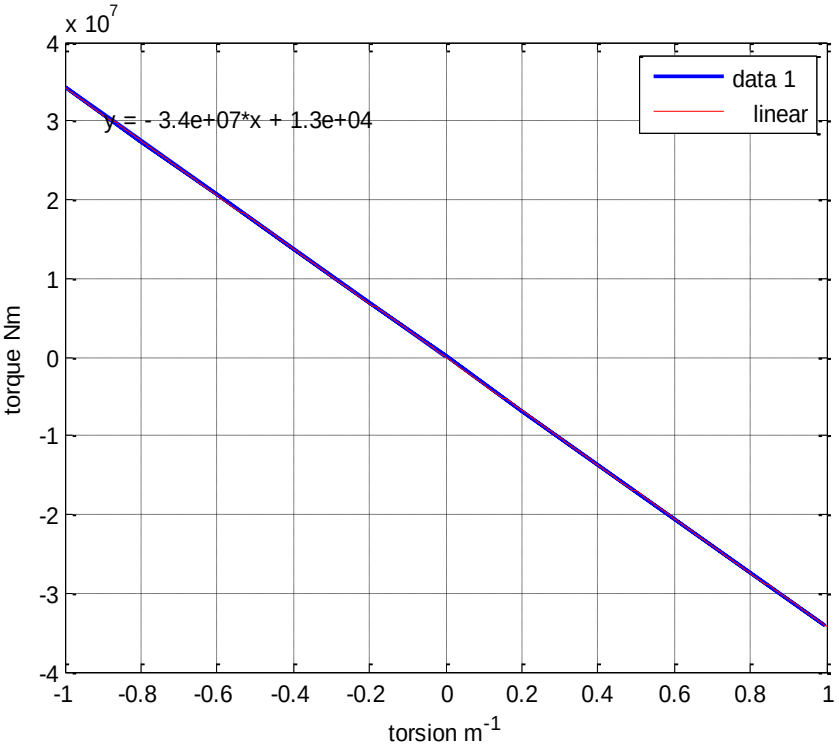

Figure 21 Torque torsion relationship

4.1.3 Influence of tension on the cross sectional characteristics

After the riser is installed, the tension force along the riser varies with the water depth. If the tension force has a large influence on the cross sectional properties, then the cross sectional properties at different water level should be defined according to the corresponding tension level. Therefore it is necessary to investigate the influence of tension force on the cross sectional properties. Since bending behavior is the main focus in this thesis, only the moment curvature relationship will be examined.

To obtain the tension force at different critical locations, a simple model was established in SIMLA with the detailed riser properties specified in section 4.2.1. The critical locations along the riser include the hang off point (A), hog (F) sag (E) part and touch down point (G), as shown in Figure 22. The tension forces at these locations in static configuration are computed and presented in Table 4.

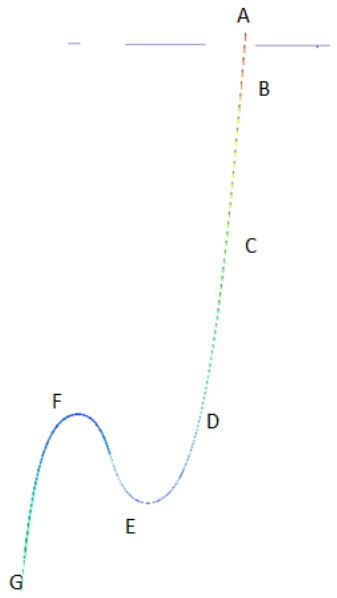

Figure 22 Critical locations along the riser

The result is verified by simple calculations. Since the riser is floating in the sea, the hogging part can be seen as lifted by the buoyancy elements. The top tension force can be regarded as

lifting the parts: AB, BC, CD, DE. The total length of this part is 323 m and the submerged weight is 272 kg/m. The top lifting force can be calculated as

$$323 \times 272 \times 9.8 = 860989N$$

The top tension given by SIMLA is 935093. The error between hand calculation and SIMLA is 8%. The result given by model in SIMLA is accepted.

Table 4 Tension force at critical locations

Point	Z	Tension
A	21.40	935093.00
B	0.49	851722.00
C	-130.40	501520.00
D	-229.76	236513.00
E	-302.22	40177.90
F	-233.44	40230.50
G	-355.00	305060.00

Next step, four critical locations along the riser A, C, D, E, are selected to be modeled in BFLEX since they represents four tension force levels. The moment curvature relationships are plotted in Figure 23.

The result shows that tension force has limited influence on the bending properties of the riser. The slip curvatures are the same for the four models. The slip moment increases with the tension force. The largest slip moment is 1.26 times of the smallest slip moment. By comparing the energy loss caused by hysteresis damping, it is found that the tension force at point A is 23 times of that at point E, however, the area of hysteresis loop at point A is only 1.5 times of the area at point E. Therefore, conclusion is drawn that the influence of tension force on the bending property of the riser could be neglected in this thesis. It is permissible to use the same moment curvature relationship to define the bending property for the whole riser. Since the hang off point endures the largest tension force, the moment curvature relationship at point A could be applied to the whole riser in the global analysis.

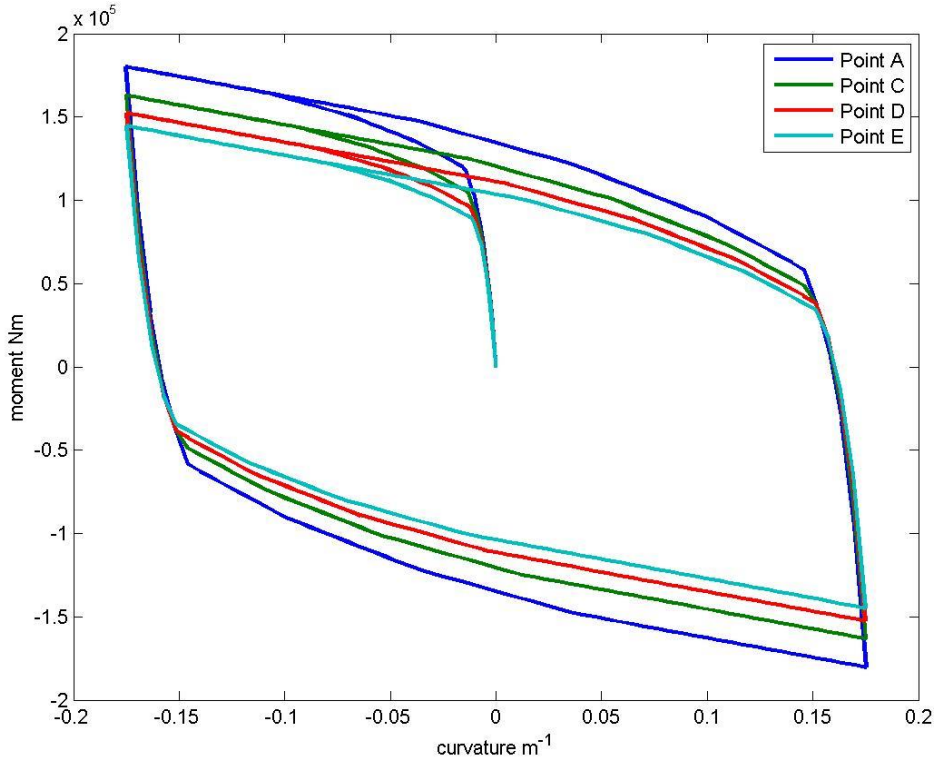

Figure 23 Influence of tension on bending property

4.2 Global analysis

The objective of global analysis of the riser is to obtain the curvature and moment responses of riser under wave loads. In this part, the global model will be established. Considering the computation capacity, the scatter diagram of the sea states will be blocked. Then the bending behavior along the riser under the representative sea blocks will be investigated.

4.2.1 Modeling of the riser

The riser is in a steep wave configuration and the main parameters are shown in Figure 24. A series of buoyancy elements is added at the lower part of the riser to lift up the riser. The riser is connected to the semi-submersible.

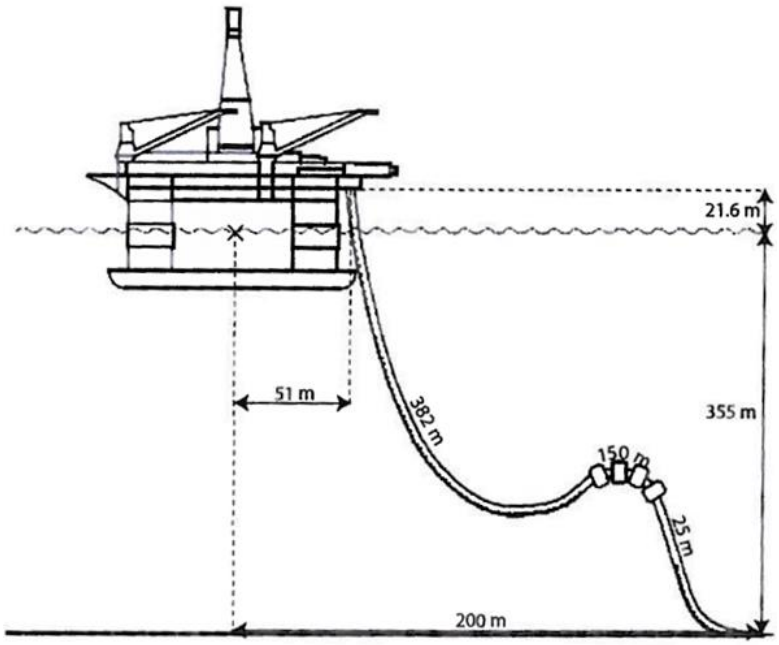

Figure 24 Riser configuration

The property of riser system is shown in Table 5 Riser properties. The bending, tension and torsional properties are based on the result of local analysis in Table 3. The moment curvature relationship plot is a tri-linear curve as shown in Figure 25.

Table 5 Riser properties

Property	Unit	Value
Length	m	565.0
Diameter	mm	401.5
Dry mass pipe	kg/m	406.5
Submerged mass pipe	kg/m	272.0
Buoyancy diameter	mm	1032.0
Dry mass buoyancy	kg/m	512.0
Submerged mass buoyancy	kg/m	-400.5
Axial stiffness	N	3.0E9
Torsional stiffness	Nm/rad	3.4E7

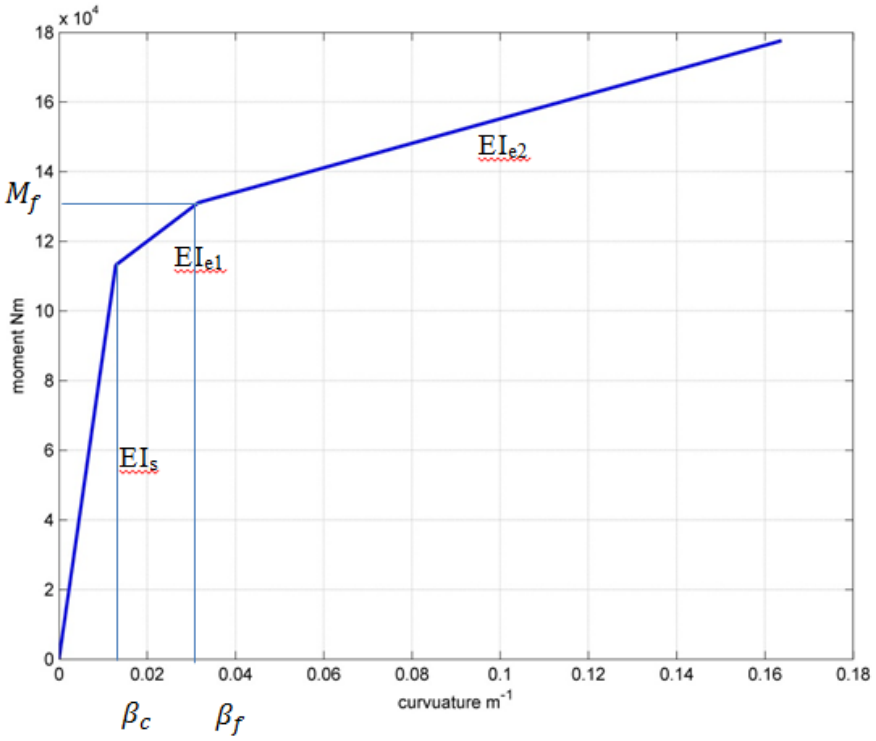

Figure 25 Moment curvature relationship

Elements and mesh

The riser is represented by 642 nodes along the riser. Node 1 is the top connection point of the riser to the vessel and node 642 is the connection point of the riser to the seabed. Element Compipe42 is used to simulate the nonlinear bending properties since Compipe42 is the elements that users could define the nonlinear material properties according to the experiment results. The mesh is finer in the hang off area than the other parts of the riser considering the significant response at the top connection.

Steps

Global analysis includes two steps. The first step is the static step to establish the initial configuration. The second step is the dynamic step to introduce waves and conduct dynamic analysis based on the static configuration.

For static analysis, the riser is originally lying on the seabed. By prescribed displacements of node 1, one end is lifted up to connect to the semi-submersible. Because of the buoyancy

elements, the riser automatically deforms into a steep wave configuration, as shown in Figure 26 .

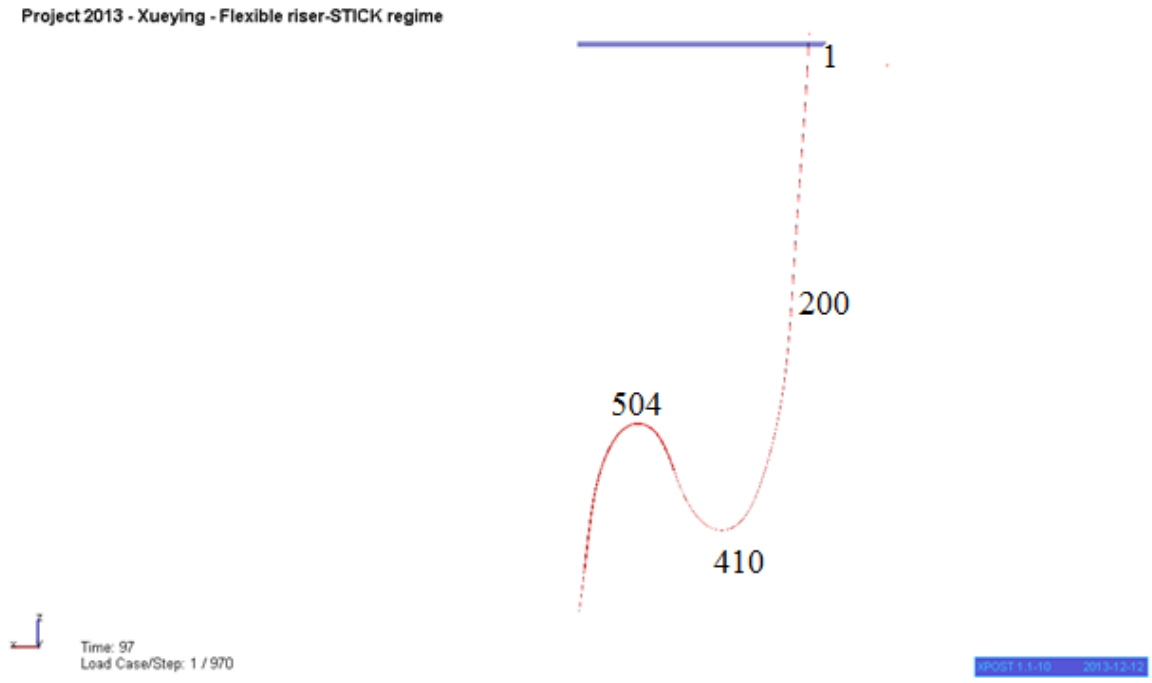

Figure 26 Model configuration

For dynamic analysis, regular waves and RAO of the semi-submsersible are introduced in the model. Node 1 of the riser is defined as the slave node of the semi-submersible so that the motion of the vessel can be transformed to the riser. In addition, the moment curvature relationship is activated in the dynamic step.

4.2.2 Test of typical global response of the riser

The sea state Hs=4m, Tp=7s is adopted to investigated the general bending properties of the riser. A large number of results can be obtained from global analysis. The most concerning results include the stress, moments, curvature distribution along the riser and their history curves.

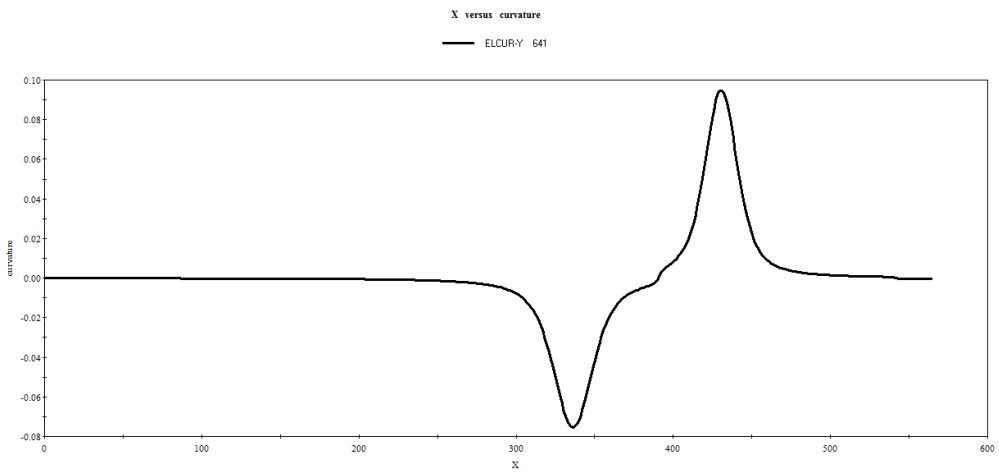

Figure 27 Global curvature distribution

The curvature distribution along the riser was obtained in Figure 27. A large curvature indicates a small radius of the curve. The curvature along the riser displays two peak values due to the steep wave configuration. The two peak values correspond to the hog and sag part of the riser repsectively.

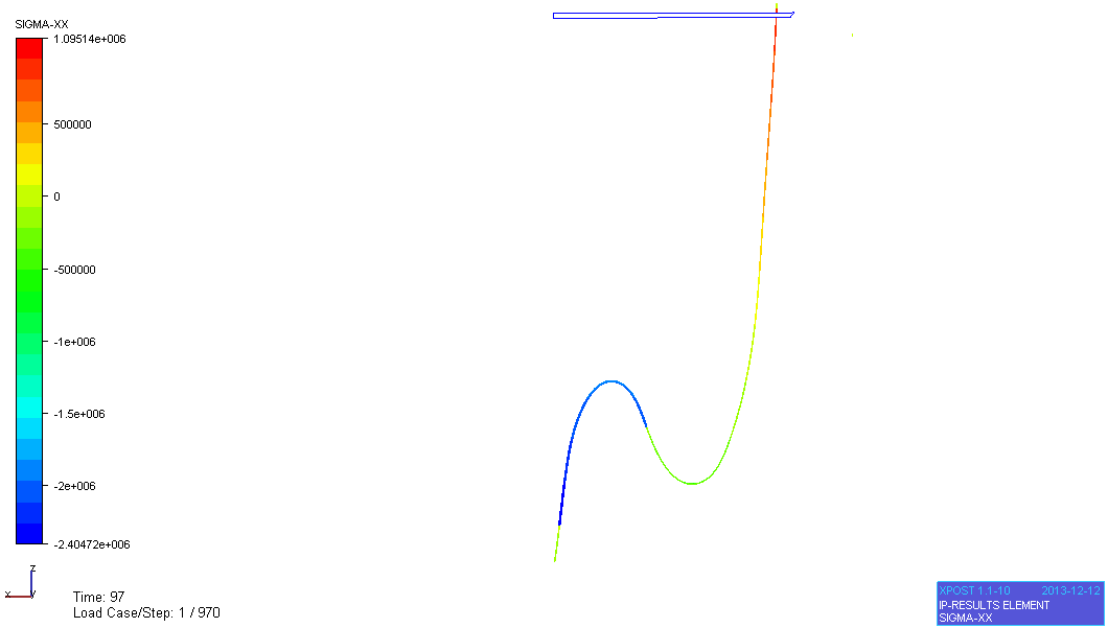

Figure 28 Stress distribution along the riser

Figure 28 shows the axial stress distribution along the riser. It is shown that a large tensile stress exists at the top connection point. The stress decreases with the increase in water depth.

However there is a large compressive stress at the buoyancy part. Compression for the pipe is dangerous since it indicates the possibility of local buckling of the pipe.

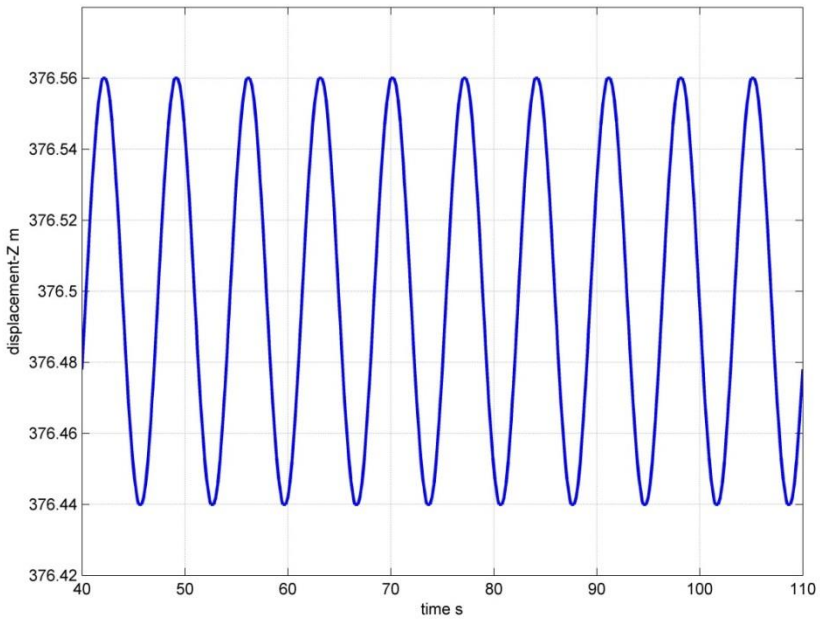

Figure 29 Displacement in vertical direction at node 1

The global response of the riser could be obtained as Figure 29. The response amplitude is controlled by the wave height and RAO. The oscillation of the riser is of the same frequency of the wave. The amplitude of vertical oscillation does not decrease with time therefore the pipe layers are kept in stick regime and there is no energy loss caused by internal friction.

Curvature history variation along the riser

Since the moment curvature relationship for the flexible riser is a tri-linear curve, the bending property in each regime is different. In order to study the behavior of the pipe under bending moment, it is preliminary to determine the curvature variations along the riser. Curvature history plots of elements at the four critical positions are drew to investigate the response along the riser, as shown in Figure 30. The element positions are illustrated as Figure 26 . Element 1 is at the hang off of riser. Element 410 and 504 are the sag and hog of the riser.

Table 6 Comparison of curvature variations along the riser

Element ID	1	200	410	504
κ_{mean}	-0,0022	-0,0003	-0,0678	0,1034
$\Delta\kappa$	0,0089	0,0012	0,0080	0,0029

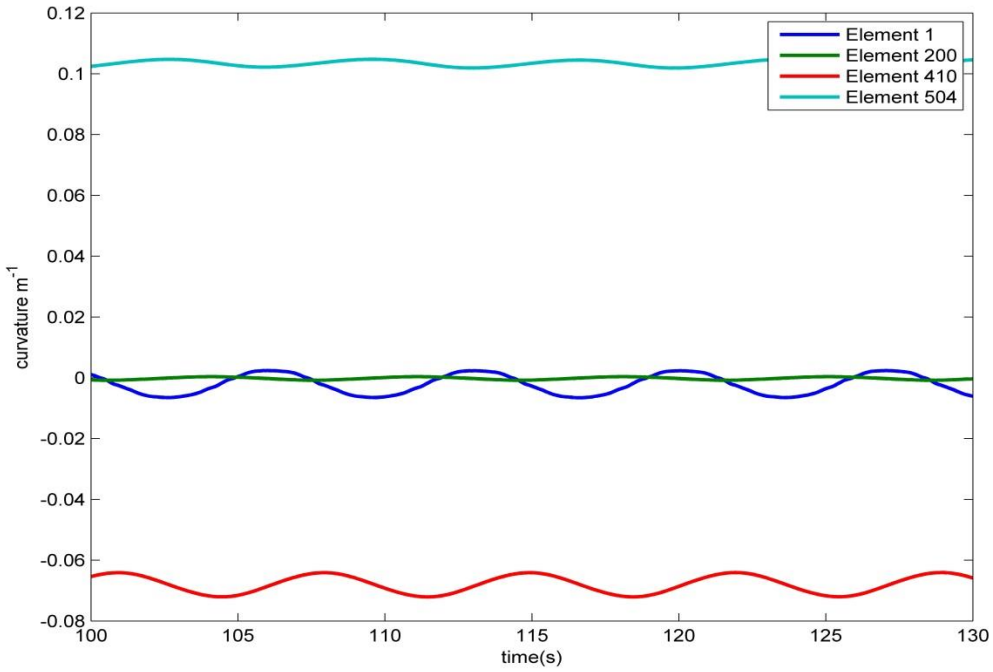

Figure 30 Curvature history plots

The mean curvatures and curvature variations at these critical points are extracted to Table 6. Element 504 has the largest mean curvature which is above 0.1 while the variation of the curvature is very small. It indicates that the response of the sag part of the riser is not significantly influenced by the wave loads. The curvature variations for element 1 and element 410 exceed 0.008, which is relatively large. However, the slip curvature for the pipeline β_c is 0.012. If slip behavior occurs between the layers of pipeline, the curvature variation must exceed twice of the slip curvature, which is 0.024. Therefore slip behavior does not occur in any positions studied above under the current sea state. The whole riser stays in the stick regime.

4.2.3 Environment condition

Sea conditions are given in a scatter diagram which contains hundreds of sea states, as in Appendix B. For regular wave analysis in this project, it is difficult to run every sea state. Therefore it is necessary to sort these sea states into blocks. Within each block, a single sea-state is selected to represent all the sea-states within the block. The probabilities of occurrence for all the sea-states within the block are lumped to the selected sea-state[24]. Each block of sea state should give similar fatigue damage to the structure.

To predict the fatigue damage to structure without really running every case, the following assumptions are made. The stress in the tensile armour, $\Delta\sigma_i$ is proportional to the curvature variation of the pipe. The curvature variation is proportional to the hang-off angle, which again is proportional to the response of the ship, ΔH_i. Therefore the fatigue damage of each block satisfies the following relationship,

$$D_i = \frac{n_i}{N_i} = \frac{n_i}{\alpha \Delta\sigma_i^{-m}} = n_i \alpha \Delta\sigma_i^{m} \propto n_i \alpha \Delta\sigma_i^{m} \propto n_i \alpha \Delta H_i^{m} \propto n_i \alpha \Delta \left(RAO * \zeta_a \right)_i^{m} \quad (4.2)$$

where ξ_a is the wave amplitude, α and m are the parameters in S-N curve. The fatigue damage D_i can be simplified as an impact value to evaluate the weighting of blocks,

$$I = \mathrm{P}\left[a \le T_p \le b, h_1 \le H_i \le h_2 \right] \Delta \overline{H}_i^{m} \quad (4.3)$$

where P is the probability of occurrence of the sea states in the block. If the value is small, it means this block of wave states can be merged with other blocks. If it is very large, then it can be further divided to achieve the evenly weighted fatigue damage.

There are two ways to conduct the first blocking of the scatter diagram: by wave periods or by wave height. By wave periods means that sorting the sea states with the same wave periods but different wave heights into one block. The representative wave height is the mean wave

height of the sea states in this block. However, this blocking gives out an over conservative result on fatigue damage prediction.

To describe the fatigue damage reasonably, it is essential to evaluate the fatigue damage contributions of both small wave height sea states and high wave height sea states. Thereby the scatter diagram should be blocked by means of wave heights.

The result of blocking scatter diagram is shown as Table 7. The parameters of each block are shown in Table 8.

Table 7 Blocked scatter diagram

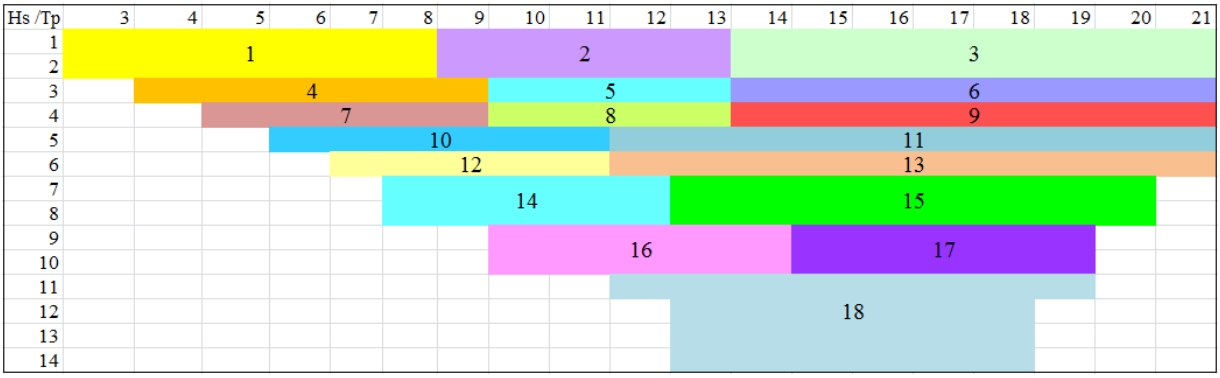

Table 8 Parameters of each block

Block ID	Hs (m)	Tp (s)	Probability	I (%)
1	1,72	6,80	0,22	0,00
2	1,86	10,27	0,18	0,02
3	1,90	15,17	0,02	0,03
4	3,00	8,00	0,12	0,00
5	3,00	11,10	0,12	0,36
6	3,00	15,10	0,02	0,26
7	4,00	8,40	0,04	0,00
8	4,00	11,20	0,09	0,90
9	4,00	15,00	0,02	0,75
10	5,00	10,03	0,05	0,13
11	5,00	13,24	0,04	3,56
12	6,00	10,37	0,02	0,14
13	6,00	13,31	0,03	5,15
14	7,23	11,37	0,01	1,51
15	7,36	14,09	0,02	8,72
16	9,20	13,10	0,00	3,22
17	9,34	15,60	0,00	2,66
18	11,20	14,80	0,00	2,06

4.2.4 Bending behavior along the riser

In this section, the responses of pipe under bending moment will be identified. In other words, the moment curvature relationships of pipes along the riser will be examined to determine when and where slip behavior will occur along the riser.

Global analysis of riser under Hs=4m, Tp=7s shows the result that slip behavior does not occur along the riser. However, the response of the riser is influence by RAO as well as the sea states. The sea state of a larger wave height or the sea state that causes resonance of the riser or vessel could lead to a much larger curvature response that may lead to the slip behavior between pipe layers.

The following sea states as shown in Table 9 are selected to examine the curvature response at different sea states. Sea states of wave height larger than 4m are examined. For small wave heights, the wave periods cover the range from 10s to 15s to include the possibility of resonance occurrence.

Table 9 Selected characteristic sea states

Block ID	Hs (m)	Tp (s)
8	4.0	15.00
10	5.0	10.03
13	6.0	13.31
15	7.4	14.09
16	9.2	13.10
18	11.2	14.80

The four critical points along the riser as in Figure 26 are again chosen to represent the curvature variations as they are considered to be the most dangerous point. The curvature variations of the points between these critical points are assumed to be within the range of the curvature variations of the neighboring critical points.

The curvature variations of the riser at four critical points under six characteristic sea states are plotted as Figure 31. Comparing the curvature variations at different sea states, it is indicated that wave height has a dominate influence on the curvature response. The increase of wave height will directly enlarge the curvature variation.

For the curvature variations along the riser under the same sea state, it is indicated that element 1, namely the hang off part of the riser, has the largest curvature variation. It is noted that the largest curvature variation (for sea states of Hs larger than 9m) even exceeds twice of the slip curvature, 0.024. At element 200, the curvature variation is almost zero since the riser is straight here. The curvature variations at element 410 and 504, namely the hog sag part, are about 0.005 to 0.01 which are still far smaller than the criterion of slip occurrence. Thereby it is concluded that slip behavior will not occur along the riser except for the hang off part.

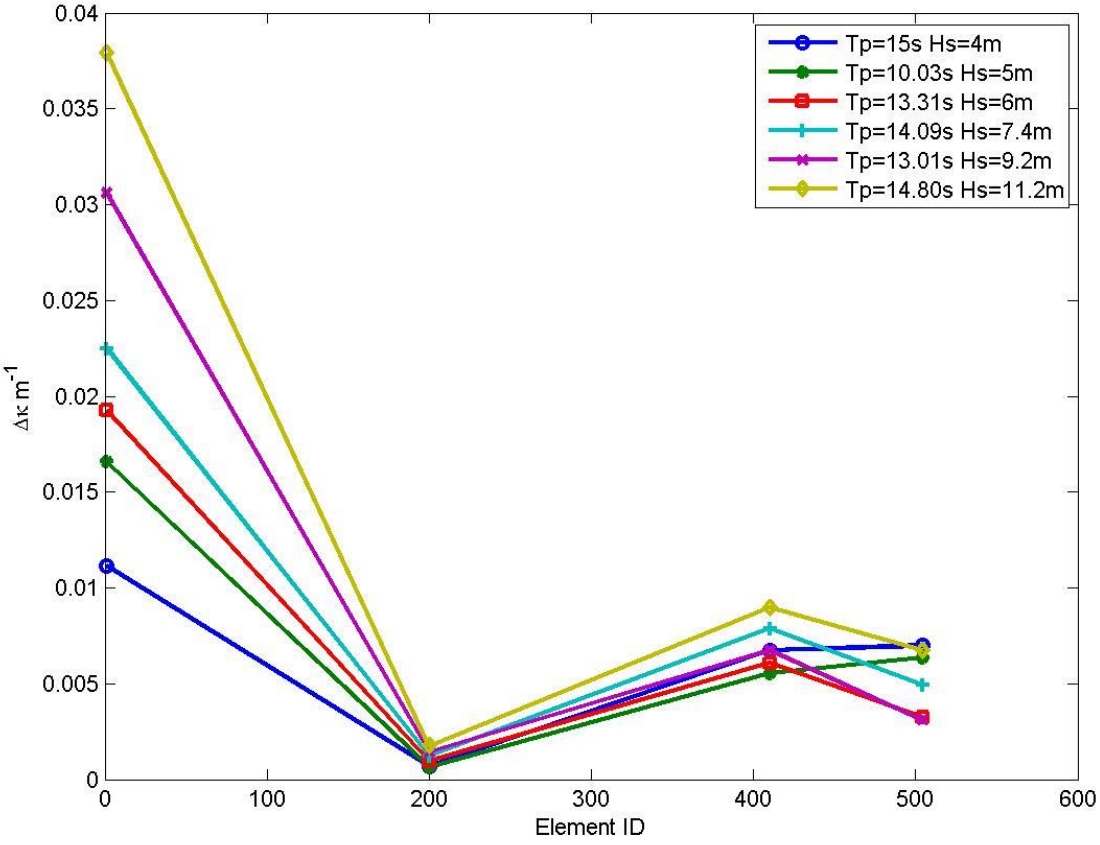

Figure 31 Curvature variations under different sea states

Then the bending behavior of element 1 under different sea states will be discussed. For wave height under 9m, the curvature variation stays below twice of the slip curvature. Therefore slip behavior does not occur between pipe layers. The moment curvature relationship for element 1 under Tp=14.09s Hs=7.4m is plotted as Figure 32. The moment varies linearly with

the curvature and the corresponding bending stiffness is 8.8E6 Nm^2, which agrees with the stick bending stiffness EI_S . Again, it is proved that the pipe layers are in the stick regime.

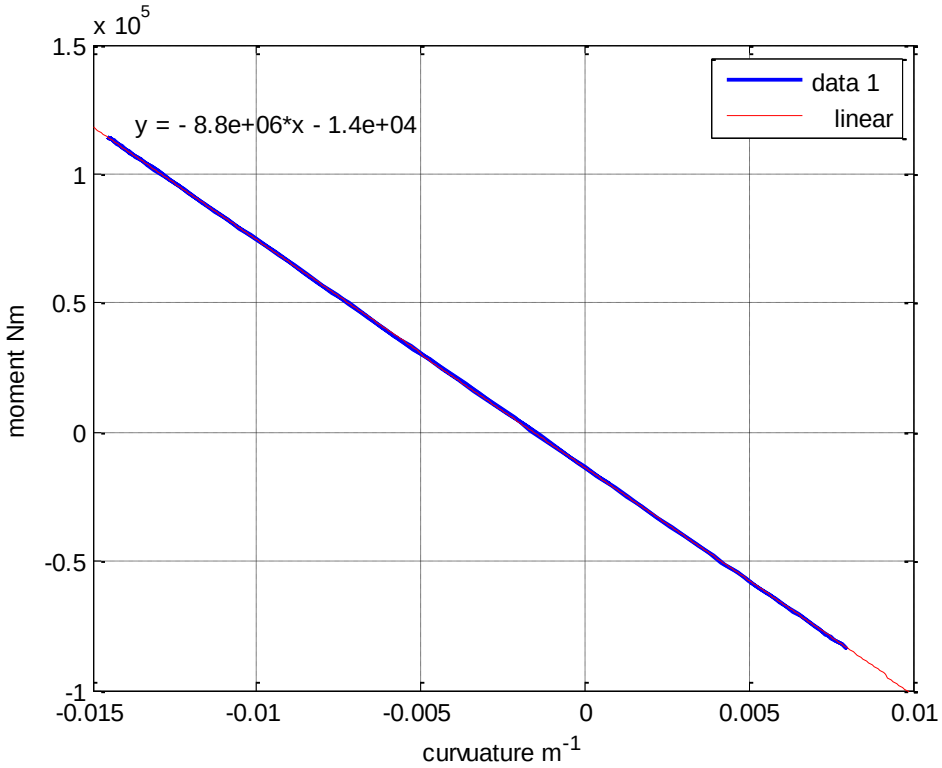

Figure 32 Moment curvature relationship for element 1 under Tp=14.09s Hs=7.4m

When the wave height is over 9m, the curvature variations at element 1 exceed 0.024. Slip initiates between layers in the pipe. From the plot of moment curvature relationship for element 1 under Tp=14.80s Hs=11.2m (Figure 33), a hysteresis loop is captured. The slopes of the curve are checked, which turns out to be the same as the stick bending stiffness EI_S and bending stiffness in the stick to slip regime EI_{e1}. Therefore it is confirmed that the layers slide relative to each other in this part of the riser.

To conclude, for the flexible pipe in this thesis, slip behavior only occurs at the hang off part of the riser when the sea environment is severe. The other parts of the riser always stay in the stick regime, i.e. the moment curvature relationship keeps being linear. Therefore the hysteresis loop only forms in the moment curvature diagram at the hang off part. It means that only at the hang off part will the internal friction force consumes energy. For the rest part of

the riser except the hang off, the energy loss due to internal friction is zero. According to equation

$$c_{eq} = \frac{W}{\pi K_0^2 \omega} \tag{2. 29}$$

the corresponding equivalent damping coefficient is zero.

The hang off part of the riser is approximately about 3 meters long and the overall length of the riser is 565 meters. In another word, Ceq is larger than zero only at the first 0.5% length of the riser. With regard to the overall riser dynamic response, the influence of hysteresis effect in the bending mode is limited. There is no need to establish the linear equivalent damping model to simulate nonlinear hysteresis damping effects for the flexible riser. Therefore the influence of linear and nonlinear damping model on the global response of the riser in the original scope will not be discussed further.

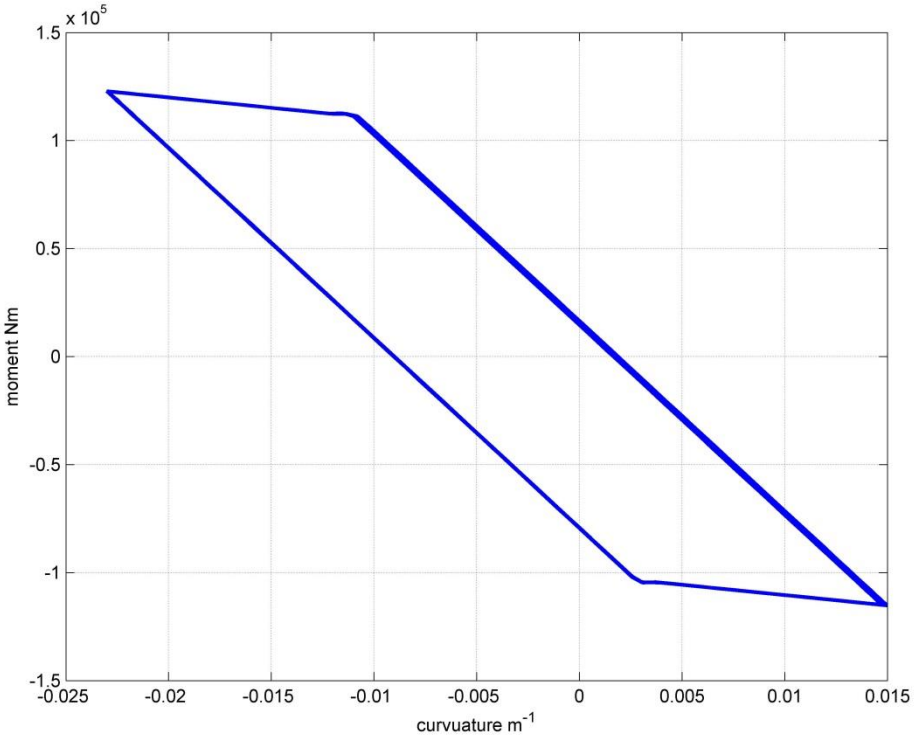

Figure 33 Moment curvature relationship for element 1 under Tp=14.80s Hs=11.2m

4.3 Summary

In this chapter, the influence of hysteresis effect in the bending mode on the global response of the riser is studied.

A pipe section model is established in BFLEX and the cross sectional characteristics of the flexible pipe are obtained. Then the global analysis of the flexible riser is performed in SIMLA based on these material properties. In the global model, the moment and curvature responses of riser at four critical locations under six representative sea states are calculated.

The result shows that slip behavior might occur in the hang off part of the riser under large wave heights. For the rest part of the riser, pipe layers stay stick to each other even under severe sea states. It means for 99.5% length of the riser, internal friction does not work to cause energy loss. Therefore for the overall flexible riser, there is no need to establish an equivalent linear damping model to simulate the nonlinear hysteresis damping effect in the bending mode.

5 Influence of Different Bending Models on Riser Responses

The moment curvature relationship of the flexible pipe under bending loads is a tri-linear curve. However in the current standard practice, a linear bending property with the bending stiffness in the full slip regime is utilized for global analysis. In this chapter, the global responses of the pipe by using linear and nonlinear bending properties will be compared.

The accumulated fatigue damage is an important degradation of riser under bending loads. Moreover, it accounts for the responses of riser in waves for a long operation period. Therefore it is used to evaluate the global response under cyclic bending loads.

As discussed previously, the nonlinearity in the moment curvature relationship only affects the hang off part. Therefore in this section, the fatigue damage results by using linear and nonlinear bending models will only be compared in the first 30 elements along the riser. The work will be carried out as follows,

- Preliminary fatigue damage analysis, including: 1) obtain the .curvature and moment responses of riser through global analysis, 2) determine the most critical point to fatigue along the riser by assuming a fictional S-N curve.
- Define the models with linear and nonlinear bending properties.
- Run lifetime analysis in Blfex for the critical pipe section based on different bending models and compare the fatigue damage results.

5.1 Preliminary fatigue damage analysis

The purpose of preliminary fatigue damage analysis is to determine the most critical point along the riser with regard to fatigue damage. The curvature and tension responses obtained in global analysis will be imposed on the pipe section as cyclic loads in fatigue analysis

5.1.1 Global analysis of the riser

Global analyses of the flexible riser under 18 blocked sea states (Table 8) utilizing the nonlinear moment curvature relationship are performed. The curvature variations of the first 30 elements along the riser are obtained (see Appendix C).

It shows that under all the sea states, the first element always has the largest curvature variation. However, typically the bending stiffener will be designed to reduce the curvature variation at the top connection and the largest curvature may occur some distance away from the connection. The explanation is that the pipes used in this thesis are heavy and with a large dimension. The length of the bending stiffener is quite small compared to the riser. Therefore even though this bending stiffener is installed at the hang off, the top connection still endures the largest curvature variation.

Comparing the curvature variations of element 1 under 18 sea states, as shown in Figure 34, the same conclusion is given as the bending behavior analysis in secion 4.2.4. A higher sea state will lead to a higher curvature variation. Curvature variations are below 0.024 m^{-1} if the the wave heights are below 9m. When wave weights are larger than the 9m, the curvature variation exceeds twice of the slip curvature.

History tension forces at the top are also recorded. The average tension force does not vary much between sea states (Figure 35), while the amplitude enlarges as the wave height grows.

So far the curvature and tension data needed for fatigue analysis has been obtained (Table 10).

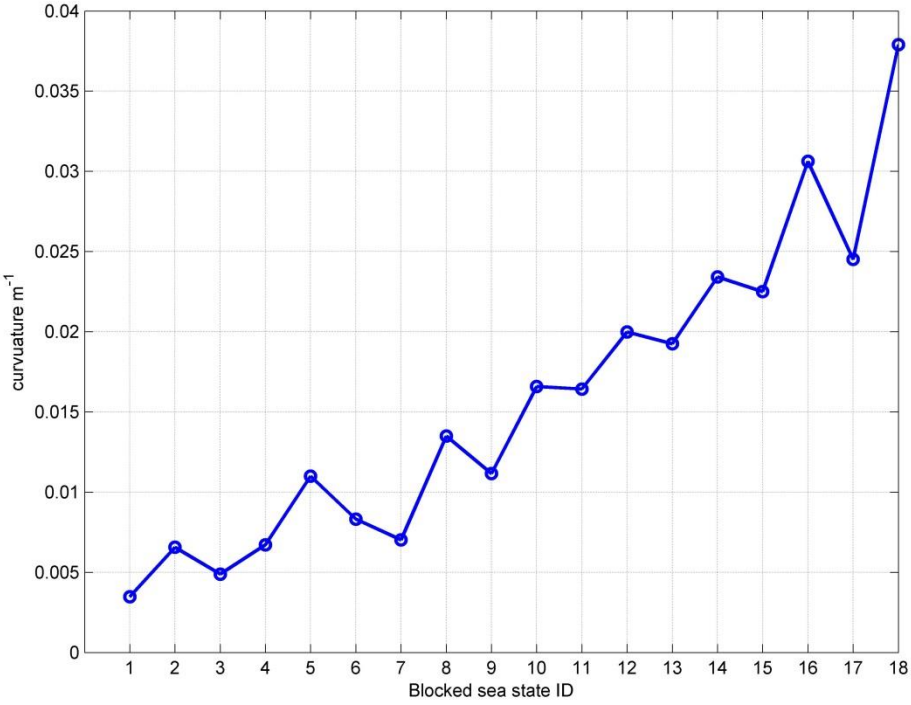

Figure 34 Curvature variations of element 1 under different sea states

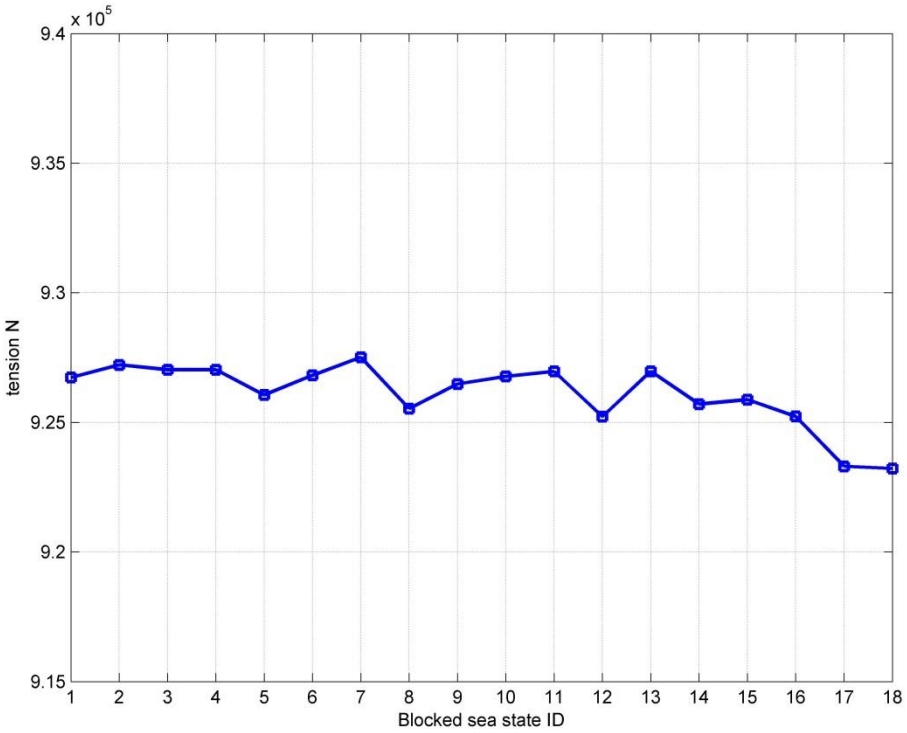

Figure 35 Mean axial force of element 1 under different sea states

Table 10 curvature variations and tension forces along the riser

Block ID	Hs(m)	Tp(s)	ni	T.min(N)	T.max(N)	T.mean(N)	△ κ
1	1.72	6.80	1005664	931046	922413	926730	0.0035
2	1.86	10.27	538440	942047	912391	927219	0.0066
3	1.90	15.17	32658	938236	915833	927035	0.0049
4	3.00	8.00	468423	929080	924981	927031	0.0067
5	3.00	11.10	340415	953743	898367	926055	0.0110
6	3.00	15.10	40245	945421	908210	926816	0.0083
7	4.00	8.40	163272	931112	923913	927513	0.0070
8	4.00	11.20	263436	963077	887980	925529	0.0135
9	4.00	15.00	36518	951776	901181	926479	0.0112
10	5.00	10.03	148309	965038	888506	926772	0.0166
11	5.00	13.24	104825	970723	883212	926968	0.0164
12	6.00	10.37	53827	972648	877793	925221	0.0200
13	6.00	13.31	72715	978279	875663	926971	0.0192
14	7.23	11.37	37360	993618	857794	925706	0.0234
15	7.36	14.09	44987	983801	867955	925878	0.0225
16	9.20	13.10	8931	1006210	844252	925231	0.0306
17	9.34	15.60	4205	983959	862649	923304	0.0245
18	11.20	14.80	1769	1004450	841989	923220	0.0379

5.1.2 Identification of the critical point of fatigue damage

The lifetime of the riser depends on the fatigue life of the most critical point along the riser. In order to investigate which point is the most critical point along the hang off part of the riser, the simplified analytical fatigue damage analysis is performed by assuming a fictional S-N curve. The procedure is as following:

1) Obtain the curvature variation ΔK_{ij} of element j under the sea state i.

2) Assuming $\Delta\kappa \propto \Delta S$ and $N=\alpha\Delta S^{-4}$, calculate the number of stress cycles to failure N_{ij} assuming a fictional S-N curve, as

$$N_{ij} = a\Delta\kappa_{ij}^{-4} \tag{5. 1}$$

3) Calculate the number of stress cycles that occurs within 1 year under the sea state i as

$$n_{ij} = \frac{3600 \times 24 \times 365}{T_{Zi}}$$

4) Compute the accumulated fatigue damage of element j from the 18 sea states as

$$D_j = \sum_{i=1}^{18} \frac{P_i n_{ij}}{N_{ij}} \qquad (5.\ 2)$$

5) Compare D_j of all the elements along the riser.

The curvature variations of the first 30 elements along the riser under 18 sea states are obtained. The fictional accumulated fatigue damage for each element is shown in Figure 36. The fatigue damage is found out to be largest at the first element.

The value of fatigue damage is not concerned here since the SN curve is an assumed curve with no design consideration.

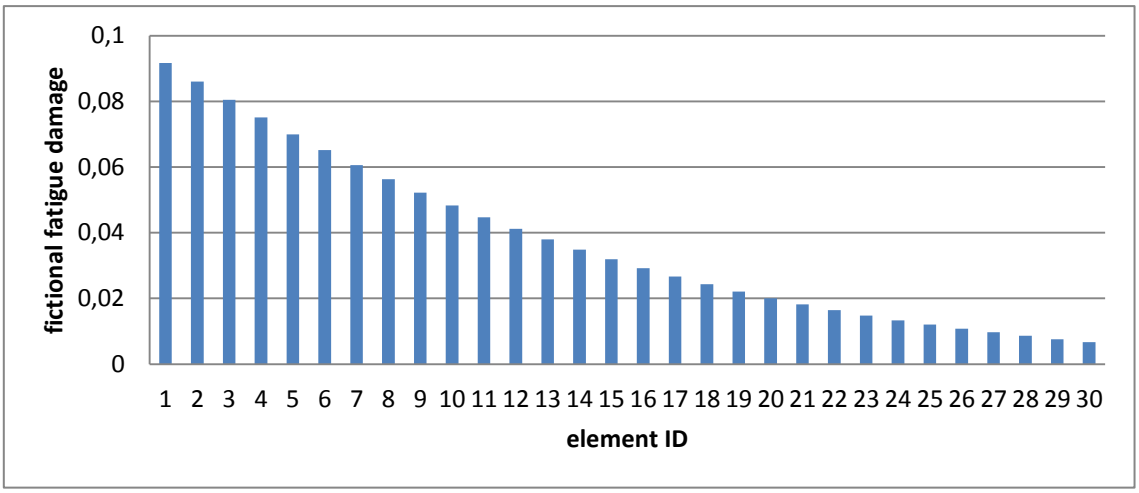

Figure 36 Fictional accumulated fatigue damage along the hang off of the riser

5.2 Definition of different damping models

To study the influence of nonlinear bending properties on the response of riser, four material models with linear and nonlinear bending stiffness are defined as Table 11.

Table 11 Linear and nonlinear damping models

Model	Material	Bending stiffness	Element
2	Nonlinear	Tri-linear moment curvature relationship (Figure 25)	COMPIPE 42
1	Linear	EI_s=8.8E6 Nm^2	PIPE 31
3	Linear	EI_{e1}=9.6E5 Nm^2	PIPE 31
4	Linear	EI_{e2}=3.5E5 Nm^2	PIPE 31

- Model 1-Nonlinear bending model: applies the nonlinear moment curvature relationship of the pipe as obtained in section 4.1.2. .
- Model 2- Stick bending model: Based on the bending stiffness of pipe in the stick regime, EI_S .
- Model 3- Stick to slip bending model: Based on the bending stiffness of pipe in the stick to slip regime, EI_{e1} .
- Model 4- Full slip bending model: Based on the bending stiffness of pipe in the slip regime, EI_{e2} .

Theoretically, model 2 and model 4 are the upper and lower boundaries for the model with nonlinear moment curvature relationship. If the global response of the riser is below twice of the slipping curvature, the pipe will be in stick regime. Then the response of the model 2 will be the same as the result given by model 1. On the other hand, if there is no friction between layers and the pipe are totally free to slip, and then the pipe can be regarded as an elastic beam. The bending stiffness will be the elastic contributions from the plastic layers and local wire bending. The result of model 1 will be identical to model 4.

5.3 Comparison between linear and nonlinear bending model

5.3.1 Lifetime Analysis Modeling

The first element is proved to be the most critical point of fatigue failure along the riser. Then this pipe section is modeled in BFLEX to conduct the real lifetime analysis. The model properties are the same as the local model in Table 2. The curvature variations and tension forces are extracted from the SIMLA model, as shown in Table 10. Curvature variation is

introduced as the time-changing prescribed rotation in the y direction. The tension force also varies with the same frequency as curvature.

The following S-N curve is adopted

$$N = a\Delta S^{-m} \tag{5. 3}$$

where $\log a = 15.1$ $m = 4$. It should be noted that these two parameters are not the design parameter for this pipeline. Therefore the lifetime data obtained has no physical meaning.

The accumulated fatigue damage distribution Based bending model 1 is presented in Figure 37. The largest fatigue damage equals to 10.5 and it occurs on the first tensile armour layer.

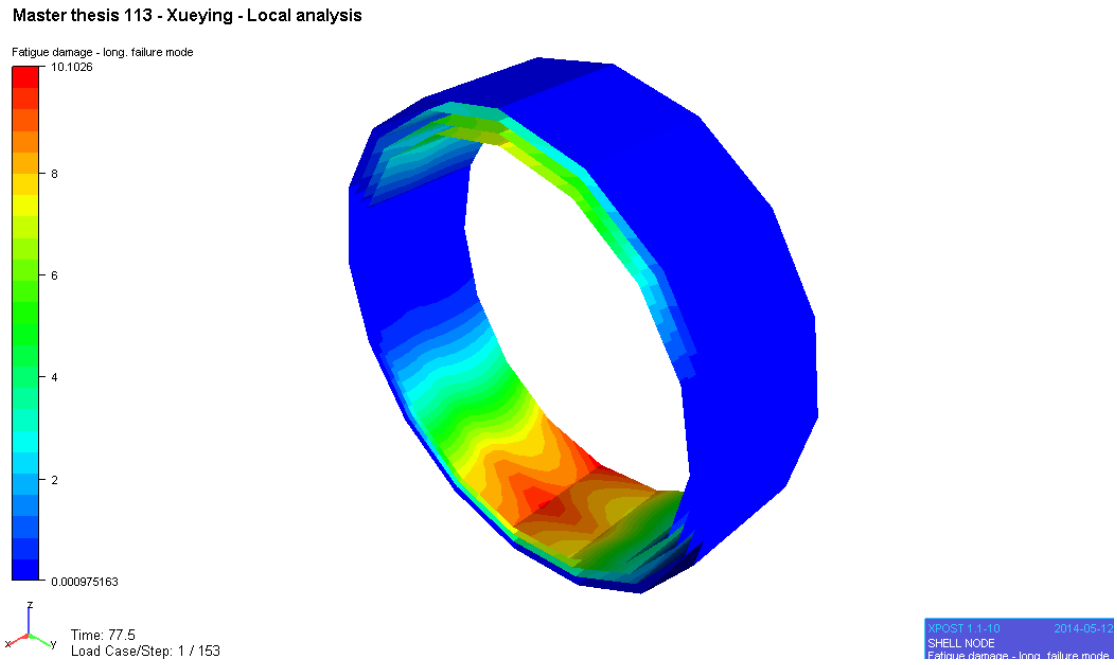

Figure 37 Fatigue damage contour

5.3.2 Global responses based different damping models

The global analyses of the four bending models are conducted to obtain the global curvature and tension responses as the inputs for lifetime analysis. The curvature variations of four models are shown in Figure 38. It is indicated that a larger bending stiffness leads to a smaller curvature variation at the hang off. This is a physical result because the higher the bending

stiffness is, the more rigid the pipe will be. Therefore under wave loads, the pipe will be less flexible to deform which results in a smaller curvature variation.

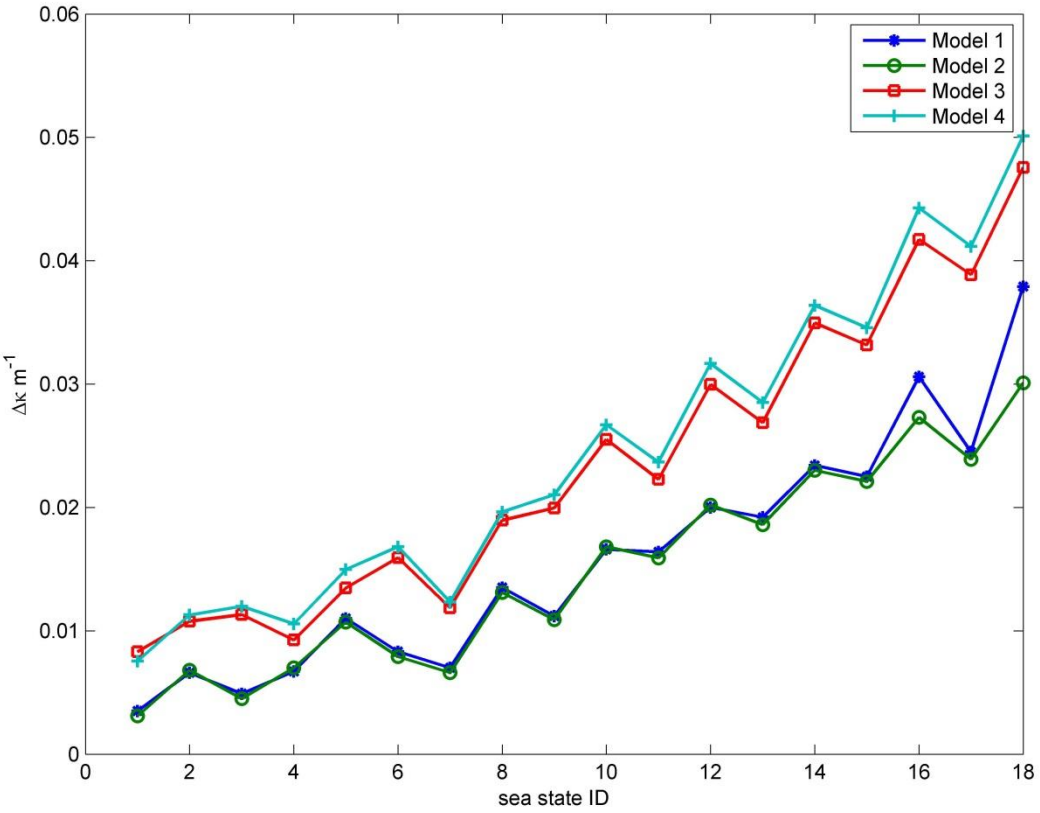

Figure 38 Curvature variations of linear and nonlinear models

The result of model 1 is very close to the result of model 2. For wave height below 9m, the pipe is in the stick regime and no slipping behavior occurs. Model 1 and model 2 give out the same result. For wave height above 9m, the layers in the pipe will start to slip and the bending stiffness reduces to EI_{e1}. Then the curvature variation given by model 1 is a little larger than that of model 2. Since the pipe experiences the process from stick to slip, the curvature variation of model 1 is still smaller than that of model 3.

5.3.3 Fatigue damage comparison

Based on the global analysis results, tension forces and curvature variations are transferred into the local model and the fatigue damage analysis are conducted for the four models. The result is illustrated as Table 12. Under the same sea environment, the fatigue damage is proportional to the curvature variation.

Table 12 Fatigue damage of four models

Model	Accumulated Damage D_i	D_i/D_2
1-Nonlinear bending model	10.1	1
2-Stick bending model	9.5	0.94
3-Stick to slip bending model	30.9	3.06
4-Full slip bending model	34.9	3.46

Model 1 is based on the real moment curvature relationship so it represents the physically correct fatigue damage prediction. Model 4, which utilizes the bending stiffness in the full slip regime, is applied for global analysis in the current standard industrial practice. By comparison, the fatigue damage given by model 4 is 3.46 times of model 2. Therefore the current utilized linear bending model gives a very conservative fatigue damage assessment.

On the other hand, the fatigue damage given by model 2, stick bending model, is 94% of the fatigue damage given by the real hysteresis bending model. Thereby, compared with the full slip bending model, the stick bending model delivers a more correct but less conservative prediction on the fatigue damage.

5.4 Summary

The full slip bending model delivers a much higher fatigue damage assessment than the real nonlinear bending model. Consequently, the current method of using a linear bending model with the bending stiffness in full slip regime for global analysis is over conservative. With the fast development of computer technology, the computation cost has been greatly reduced. To

obtain a more exact fatigue damage assessment, it is advisable to conduct the global analysis with the real nonlinear moment curvature relationship.

As discussed in section 4.2.4, slip behavior between layers in the flexible pipes only occurs under very severe sea states. In most cases, the wires will be in the stick regime instead of the slip regime. Therefore if a linear bending model is to be applied, it is recommended to use the bending stiffness in the stick regime and introduce a proper safety factor for the global analysis. The determination of the safety factor should be studied more extensively.

6 Conclusions and Recommendations

The thesis studies the bending behavior of flexible pipes with focuses on two topics: 1) hysteresis effects in the bending mode 2) influence of linear and nonlinear bending models. The following conclusions can be drawn:

1) Hysteresis damping in the bending mode has limited effect on the global response of riser, which excludes the necessity to further study the equivalent damping models. It is found that slip behavior only occurs only at the hang off part of the riser. For the rest part, pipe layers stay in the stick regime, meaning there is no energy loss due to internal friction.

2) The current industrial practice, i.e. applying the linear damping model with the full slip bending stiffness in the global riser analysis, gives an over conservative assessment of the fatigue damage. Thereby it is recommended to apply the real nonlinear moment curvature bending relationship in the global analysis. If a linear bending model is to be utilized, it is more reasonable to use the bending stiffness in the stick regime and applying a proper safety factor.

The conclusions obtained above are limited to the current case. In order to generalize the conclusion, the following issues are recommended to be further studied:

1) The bending behaviors of more pipelines should be investigated in order to give a widely applicable conclusion. The bending behavior of the flexible pipes is unique for each pipeline design. It is necessary to test if the conclusions obtained in this thesis are the common rules for flexible pipes.

2) It is recommended to apply the stick bending stiffness instead of the slip bending stiffness if a linear bending model is to be used in the global analysis. Meanwhile a proper safety factor is required to be applied. The determination of the safety factor should be based on a wide range of case studies.

Reference

1. Thorsen, M.J., *Capacity of Deep Water Flexible Risers*. 2011.
2. Sævik, S., *Theoretical and experimental studies of stresses in flexible pipes.* Computers & Structures, 2011. **89**(23): p. 2273-2291.
3. *API-RP-17B. Recommended practice for flexible pipe*. 1998, American Petroleum Institute.
4. Sævik, S., *Lecture Notes in Offshore Pipeline Technology*. 2013.
5. Sævik, S., *Handbook on Design and Operation of Flexible Pipes.* 2013.
6. Bai, Y. and Q. Bai, *Subsea engineering handbook*. 2012: Gulf Professional Publishing.
7. Andersen, M., A. Berg, and S. Saevik. *Development of an optical monitoring system for flexible risers*. in *Offshore Technology Conference*. 2001. Offshore Technology Conference.
8. Sævik, S., *A finite element model for predicting stresses and slip in flexible pipe armouring tendons.* Computers & Structures, 1993. **46**(2): p. 219-230.
9. Sævik, S., *On stresses and fatigue in flexible pipes.* 1992.
10. Saevik, S., *Bflex2010-Theory Manual*. 2010, MARINTEK.
11. Skallerud, B., *Damping models and structural damping in a nonbonded pipe*. 1991, SINTEF.
12. Sævik, S. and R.T. Igland. *Calibration of a flexible pipe tensile armour stress model based on fibre optic monitoring*. in *ASME 2002 21st International Conference on Offshore Mechanics and Arctic Engineering*. 2002. American Society of Mechanical Engineers.
13. Sævik, S. *Comparison Between Theoretical and Experimental Flexible Pipe Bending Stresses*. in *ASME 2010 29th International Conference on Ocean, Offshore and Arctic Engineering*. 2010. American Society of Mechanical Engineers.
14. Sævik, S., E. Giertse, and G. Olsen. *A new method for calculating stresses in flexible pipe tensile armours*. in *OMAE 1998: 17 th International Conference on Offshore Mechanics and Arctic Engineering*. 1998.
15. Zhao, B., *Fatigue Analysis of Flexible Riser-Effect of Mean Stress Correction Procedures.* 2013.
16. *DNV-RP-C203: Fatigue design of offshore steel structures*. 2005, Det Norsk Veritas.
17. Saevik, S. and S. Berge, *Fatigue testing and theoretical studies of two 4 in flexible pipes.* Engineering Structures, 1995. **17**(4): p. 276-292.
18. Sævik, S. and M.J. Thorsen. *Techniques for Predicting Tensile Armour Buckling and Fatigue in Deep Water Flexible Pipes*. in *ASME 2012 31st International Conference*

on Ocean, Offshore and Arctic Engineering. 2012. American Society of Mechanical Engineers.

19. Saevik, S., *Simla-Theory Manual*. 2010, MARINTEK.
20. Sævik, S., L. Gray, and A. Phan. *A Method for Calculating Residual and Transverse Stress Effects in Flexible Pipe Pressure Spirals*. in *Proceedings of the 20th International Conference on Offshore Mechanics and Arctic Engineering (OMAE 2001 CD)*. 2001.
21. Sævik, S. and H. Li. *Shear Interaction and Transverse Buckling of Tensile Armours in Flexible Pipes*. in *ASME 2013 32nd International Conference on Ocean, Offshore and Arctic Engineering*. 2013. American Society of Mechanical Engineers.
22. Saevik, S., *Bflex2010-Usermanual*. 2010, MARINTEK.
23. Saevik, S., *Simla-Usermanual*. 2010, MARINTEK.
24. *DNV-RP-F204: Riser Fatigue*. 2010, Det Norske Veritas.

Appendix

Appendix A – Pipe Data

The pipe data is expressed as below:

water depth	355				
Internalpressure	47,5 Mpa				
Layer	Thickness(mm)	Material	I.D. (mm)	weight(kg/m)	Lay angle
Carcass	7	Steel	228,6	23,786	88,588753
Antiwear	3,99	PVDF	242,6	4,097	
Barrier	12	PVDF	248,6	17,389	
Antiwear	1,02	PVDF	272,6	0,873	
Z-spiral	12	Carbon Steel	274,63	68,762	89,417383
Flat spiral	5,99	Carbon Steel	298,63	40,835	86,499369
Antiwear	1,52	PA11(nylon)	310,62	1,569	
Tensile armour 1	5,99	Carbon Steel	313,67	43,049	44
Antiwear	0,41	PA11(nylon)	325,66	0,425	
Antiwear	1,52	PA11(nylon)	326,47	1,649	
Tensile armour 2	5,99	Carbon Steel	329,53	45,4	44
Antiwear	0,41	PA11(nylon)	341,51	0,445	
Antiwear	1,52	PA11(nylon)	342,32	1,729	
Tensile armour 3	5,99	Carbon Steel	345,37	46,991	42
Antiwear	0,41	PA11(nylon)	357,36	0,466	
Antiwear	1,52	PA11(nylon)	358,17	1,808	
Tensile armour 4	5,99	Carbon Steel	361,22	49,265	-42
Antiwear	0,41	PA11(nylon)	373,21	0,487	
Antiwear	1,52	PA11(nylon)	374,02	0,319	
Protective shealth	12	PA11(nylon)	374,83	15,312	

The steel tendon cross-section details are summarized as below.

Layer	Dimension (mm)	Pitch (mm)	Wires	Angle (°)	filled
Carcass	55x1,4	-	-	-	-
Z-spiral	26,8x12	-	-	-	-
Flat spiral	16x6	-	1	-	-
Tensile armour 1	12x6	1039,9	54	44	91,3
Tensile armour 2	12x6	1091,5	57	44	91,8
Tensile armour 3	12x6	1225,9	61	42	90,7
Tensile armour 4	12x6	1281,2	64	42	91,0

Material properties are shown as

Material	Young's modulus (MPa)	Possion's ratio
Steel	2e5	0,3
Plastic layers	300	0,4

Geometry of bending stiffener is illustrated as

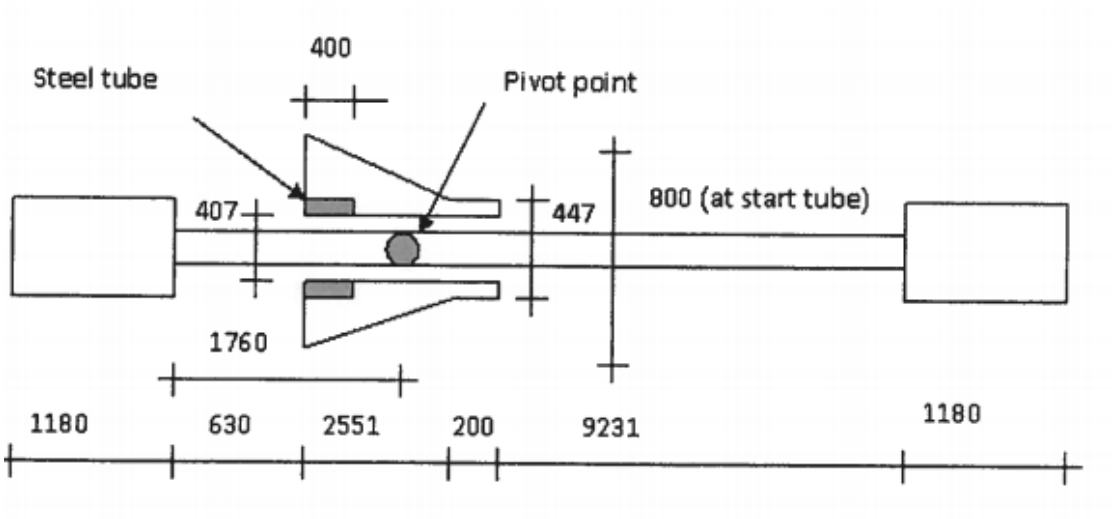

Appendix B-Scatter Diagram

Scatter diagram of sea environment

Hs /Tp	3	4	5	6	7	8	9	10	11	12	13	14	15	16	17	18	19	20	21	
1	59	403	1061	1569	1634	1362	982	643	395	232	132	74	41	22	12	7	4	2	2	8636
2	9	212	1233	3223	5106	5814	5284	4102	2846	1821	1098	634	355	194	105	56	30	16	17	32155
3		8	146	831	2295	3896	4707	4456	3531	2452	1543	901	497	263	135	67	33	16	15	25792
4			6	85	481	1371	2406	2960	2796	2163	1437	849	458	231	110	50	22	10	7	15442
5				4	57	315	898	1564	1879	1696	1228	748	398	191	84	35	13	5	3	9118
6					3	39	207	571	950	1069	885	575	309	142	58	21	7	2	1	4839
7						2	27	136	347	528	533	387	217	98	37	12	4	1		2329
8							2	20	88	197	261	226	138	64	23	7	2			1028
9								2	15	54	101	111	78	39	14	4	1			419
10									2	11	30	45	39	22	8	2	1			160
11										2	7	15	16	11	5	1				57
12											1	4	6	5	2	1				19
13												1	2	2	1					6
14														1						1
15																				0
		68	623	2446	5712	9576	12799	14513	14454	12849	10225	7256	4570	2554	1285	594	263	117	52	45	1E+05

Appendix C-Curvature Response

The curvature variations of the first elements along the riser under 18 sea blocks:

Sea Block	Ihs	tp	probabilitni	element	2	3	4	5	6	7	8	9	10	11	12	13	14
1,00000	1,72000	6,80000	0,21685	0,00347	0,0034	0,00338	0,00333	0,00328	0,00322	0,00317	0,00311	0,00306	0,00300	0,00294	0,00288	0,00282	0,00277
2,00000	1,86000	10,27000	0,17535	538440	0,0065	0,00637	0,00628	0,00618	0,00608	0,00598	0,00587	0,00577	0,00566	0,00555	0,00544	0,00533	0,00521
3,00000	1,89500	15,17000	0,01571	32658	0,0048	0,00475	0,00468	0,00460	0,00453	0,00445	0,00437	0,00429	0,00421	0,00413	0,00405	0,00397	0,00388
4,00000	3,00000	8,00000	0,11883	468423	0,0066	0,00651	0,00641	0,00630	0,00620	0,00608	0,00597	0,00586	0,00574	0,00563	0,00551	0,00539	0,00527
5,00000	3,00000	11,10000	0,11982	340415	0,0108	0,01069	0,01053	0,01036	0,01019	0,01002	0,00984	0,00967	0,00949	0,00930	0,00912	0,00893	0,00874
6,00000	3,00000	15,10000	0,01927	40245	0,0082	0,00808	0,00796	0,00783	0,00771	0,00758	0,00744	0,00731	0,00717	0,00703	0,00689	0,00675	0,00661
7,00000	4,00000	8,40000	0,04349	163272	0,0069	0,00681	0,00670	0,00659	0,00648	0,00636	0,00624	0,00612	0,00600	0,00588	0,00575	0,00563	0,00550
8,00000	4,00000	11,20000	0,09356	263436	0,0133	0,01311	0,01292	0,01272	0,01251	0,01230	0,01208	0,01186	0,01164	0,01141	0,01119	0,01096	0,01073
9,00000	4,00000	15,00000	0,01737	36518	0,0110	0,01084	0,01068	0,01051	0,01034	0,01017	0,00999	0,00981	0,00962	0,00944	0,00925	0,00906	0,00887
10,00000	5,00000	10,03000	0,04717	148309	0,0164	0,01612	0,01587	0,01563	0,01537	0,01511	0,01485	0,01458	0,01430	0,01402	0,01374	0,01346	0,01318
11,00000	5,00000	13,24000	0,04401	104825	0,0162	0,01597	0,01573	0,01549	0,01523	0,01498	0,01472	0,01445	0,01418	0,01391	0,01363	0,01335	0,01307
12,00000	6,00000	10,37000	0,01770	53827	0,0197	0,01943	0,01913	0,01883	0,01853	0,01821	0,01789	0,01757	0,01724	0,01691	0,01657	0,01623	0,01589
13,00000	6,00000	13,31000	0,03069	72715	0,0190	0,01871	0,01843	0,01815	0,01785	0,01755	0,01725	0,01694	0,01662	0,01630	0,01598	0,01565	0,01532
14,00000	7,23000	11,37000	0,01347	37360	0,0231	0,02276	0,02242	0,02207	0,02171	0,02135	0,02097	0,02059	0,02021	0,01982	0,01943	0,01903	0,01863
15,00000	7,36000	14,09000	0,02010	44987	0,0222	0,02188	0,02155	0,02121	0,02087	0,02052	0,02016	0,01980	0,01943	0,01905	0,01868	0,01830	0,01791
16,00000	9,20000	13,10000	0,00371	8931	0,0297	0,02865	0,02761	0,02661	0,02593	0,02547	0,02503	0,02457	0,02412	0,02365	0,02319	0,02272	0,02224
17,00000	9,34000	15,60000	0,00208	4205	0,0242	0,02382	0,02347	0,02310	0,02272	0,02234	0,02195	0,02155	0,02115	0,02074	0,02033	0,01992	0,01950
18,00000	11,20000	14,80000	0,00083	1769	0,0369	0,03580	0,03458	0,03329	0,03192	0,03047	0,02899	0,02755	0,02624	0,02560	0,02510	0,02459	0,02408

15	16	17	18	19	20	21	22	23	24	25	26	27	28	29	30
0,00271	0,0026	0,0026	0,003	0,0025	0,0024	0,00235	0,00229	0,00223	0,00217	0,00212	0,00206	0,00201	0,00195	0,00189	0,00183
0,00510	0,0050	0,0049	0,005	0,0046	0,0045	0,00443	0,00432	0,00421	0,00410	0,00399	0,00389	0,00378	0,00367	0,00356	0,00345
0,00380	0,0037	0,0036	0,004	0,0035	0,0034	0,00330	0,00321	0,00313	0,00305	0,00297	0,00289	0,00282	0,00273	0,00265	0,00257
0,00515	0,0050	0,0049	0,005	0,0047	0,0046	0,00443	0,00432	0,00420	0,00409	0,00398	0,00386	0,00375	0,00364	0,00352	0,00341
0,00855	0,0084	0,0082	0,008	0,0078	0,0076	0,00742	0,00724	0,00705	0,00687	0,00669	0,00652	0,00634	0,00616	0,00597	0,00579
0,00647	0,0063	0,0062	0,006	0,0059	0,0058	0,00561	0,00547	0,00533	0,00519	0,00506	0,00493	0,00479	0,00466	0,00451	0,00437
0,00538	0,0053	0,0051	0,005	0,0049	0,0048	0,00463	0,00451	0,00439	0,00427	0,00415	0,00403	0,00392	0,00380	0,00368	0,00356
0,01049	0,0103	0,0100	0,010	0,0096	0,0093	0,00911	0,00888	0,00866	0,00843	0,00822	0,00800	0,00779	0,00756	0,00733	0,00710
0,00867	0,0085	0,0083	0,008	0,0079	0,0077	0,00753	0,00734	0,00716	0,00697	0,00679	0,00661	0,00644	0,00625	0,00606	0,00587
0,01289	0,0126	0,0123	0,012	0,0118	0,0115	0,01119	0,01091	0,01063	0,01036	0,01009	0,00982	0,00956	0,00929	0,00900	0,00872
0,01279	0,0125	0,0122	0,012	0,0117	0,0114	0,01111	0,01084	0,01056	0,01029	0,01003	0,00976	0,00950	0,00923	0,00895	0,00868
0,01555	0,0152	0,0149	0,015	0,0142	0,0138	0,01349	0,01316	0,01283	0,01250	0,01217	0,01185	0,01153	0,01120	0,01086	0,01052
0,01499	0,0147	0,0143	0,014	0,0137	0,0133	0,01302	0,01270	0,01238	0,01206	0,01175	0,01144	0,01114	0,01082	0,01049	0,01017
0,01823	0,0178	0,0174	0,017	0,0166	0,0162	0,01583	0,01544	0,01505	0,01466	0,01428	0,01391	0,01354	0,01315	0,01275	0,01236
0,01753	0,0171	0,0168	0,016	0,0160	0,0156	0,01522	0,01484	0,01447	0,01410	0,01373	0,01337	0,01302	0,01264	0,01226	0,01188
0,02177	0,0213	0,0208	0,020	0,0199	0,0194	0,01892	0,01845	0,01799	0,01753	0,01708	0,01663	0,01619	0,01573	0,01525	0,01479
0,01908	0,0187	0,0182	0,018	0,0174	0,0170	0,01657	0,01616	0,01575	0,01535	0,01495	0,01456	0,01417	0,01377	0,01335	0,01294
0,02356	0,0230	0,0225	0,022	0,0215	0,0210	0,02048	0,01997	0,01947	0,01897	0,01848	0,01800	0,01752	0,01702	0,01650	0,01600